Phylogenetics and biogeography of two new species of paromomyid plesiadapiforms from a unique, High Arctic ecosystem of Eocene Canada

By

Kristen Miller
B.A., Colorado State University, 2018

Submitted to the graduate degree program in Ecology and Evolutionary Biology and the Graduate Faculty of the University of Kansas in partial fulfillment of the requirements for the degree of Master of Arts.

Chair: Dr. K. Christopher Beard

Dr. Kelly Matsunaga

Dr. Jaelyn Eberle

Date Defended: 5 May 2021

The thesis committee for Kristen Miller certifies that this is the approved version of the following thesis:

Phylogenetics and biogeography of two new species of paromomyid plesiadapiforms from a unique, High Arctic ecosystem of Eocene Canada

Chair: Dr. K. Christopher Beard

Date Approved: May 2021

Abstract

The Margaret formation of the Eureka Sound Group in the Canadian Arctic Archipelago samples a unique, warm temperate ecosystem with a polar light regime that dates to the early Eocene epoch ~ 53 Ma. Previous paleontological expeditions into this region have yielded a wide array of vertebrate taxa including early crocodilians and a diversity of mammals. Although crown clade primates have never been recovered from the Eocene of Arctic Canada, at least two new taxa of paromomyid plesiadapiforms occur there. This research aims to describe the Arctic paromomyids from Ellesmere Island and assess their phylogenetic relationships with respect to other members of this clade with the goal of reconstructing the paleobiogeographic affinities of these arboreal taxa and constraining the timing by which they colonized the Canadian Arctic. A phylogenetic analysis was completed using a morphological character matrix utilizing 63 dental characters scored for 17 taxa. A parsimony analysis completed using PAUP* suggests the two new paromomyid species are sister taxa that are highly nested within the *Ignacius* clade. These results suggest the Arctic paromomyids are closely related to mid-latitude North American paromomyid clades and are not specially related to the European genus *Arcius*. The nested relationship also suggests the Arctic taxa dispersed into high northern latitudes after the initial diversification of North American paromomyids during the Paleocene.

The date for the lower faunal zone of the Margaret Formation (where most of the mammalian taxa occur) coincides with increasing temperatures during the Early Eocene Climatic Optimum (EECO). This suggests the northerly dispersal of the Arctic paromomyids may have been in response to rising global temperatures during the EECO. Further research on the new taxa will be focused on dental topography analysis to better understand the ecological adaptations that allowed for their survival in an ecosystem with a polar light regime.

Acknowledgments

First, I would like to thank the late Mary Dawson for her persistence and dedication in documenting the unique fauna of the Canadian Arctic and the decades of field work she conducted alongside Howard Hutchison, Malcom McKenna, Jaelyn Eberle, and others. I would like to thank the Canadian Museum of Nature for loaning the study material for my research as well as the University of Colorado Museum of Natural History for loaning comparative specimens.

I would also like to thank my committee members Jaelyn Eberle and Kelly Matsunaga for their feedback, advice, and encouragement throughout the duration of my thesis project. Additionally, I would also like to thank Jaelyn Eberle for sharing her extensive and invaluable knowledge pertaining to the geology, localities, and fauna of Ellesmere Island and the Canadian Arctic. I would especially like to thank my advisor, Chris Beard for offering this project for my thesis research as well as for his continued guidance, advice, and encouragement throughout this project. I am indebted to my fellow lab mates Spencer Mattingly, Matt Jones, Chenchen Shen, and Kathleen Rust for sharing their knowledge and offering guidance and advice, as well as scientific illustrator, Kristen Tietjen for her assistance in generating figures for my thesis. Additionally, I would like to thank Oscar Sanisidro for assisting with micro-CT scanning of the fossil specimens used in this research.

I would like to thank the David B. Jones Foundation and the Association of Earth Sciences Clubs of Greater Kansas City for their financial support as well as the University of Kansas Biodiversity Institute for providing funding for this research through the Panorama Grant.

I would like to thank my friends and fellow graduate students, Rachel Neff, Kathleen Rust, Ben Kerbs, Isabel Pen, Ceyda Kural, and Keana Tang for their comradery, support, never-ending encouragement, Sunday dinners, and study nights. I would not have been able to do this without you. Additionally, I would like to thank my undergraduate mentors Kimberly Nichols and Thomas Bown for inviting me to participate in three years of paleontological field work that sparked my passion for early Cenozoic paleontology as well as providing unending support to prepare me for graduate school.

Finally, I would like to thank my parents, Shari and Bill for their unconditional support and I would especially like to thank my sister, Megan for sharing her contagious passion for biology and natural history and her unconditional love and encouragement. Last, but not least, I am forever grateful for my dog, Pippin for the persistent, daily reminders to take breaks.

Table of Contents

List of Figures

List of Tables

1. Introduction

The Paleocene and early Eocene epochs (ca. 66-50 Ma) are especially important intervals of time for understanding the radiation of early placental mammal clades. The onset of the Paleocene Epoch after the end Cretaceous mass extinction resulted in an ecosystem with newly vacant niches providing the opportunity for mammals to radiate and diversify (Alroy 1999; Rose 2006). Many important placental mammal clades have origins in the Late Cretaceous and early Paleogene, including rodents, carnivorans, 'condylarths' (commonly called archaic ungulates), and plesiadapiforms, extinct members of the clade Primatomorpha which includes the extant orders Primates and Dermoptera (Lillegraven and Eberle 1999; Rose 2006; Wilson et al. 2021).

The boundary between the Paleocene and Eocene epochs, around 56 million years ago (Foreman et al. 2012), is marked by a significant carbon isotope excursion reflecting a rapid global warming event lasting approximately 200,000 years known as the Paleocene-Eocene Thermal Maximum (PETM) (Foreman et al. 2012; Kraus et al. 2013). The PETM separates the cooler, dryer climate of the Paleocene from the warmer, humid climate of the Eocene (Kraus et al. 2013), and marks a faunal turnover event where many of the common mammalian taxa of the Paleocene are replaced by new mammal clades, many of which still exist today, including perissodactyls, artiodactyls, and primates (Rose 2006).

One group of mammals which successfully traverses the PETM is the plesiadapiforms. The phylogenetic relationships of plesiadapiforms is still highly contested in the literature. Some researchers consider plesiadapiforms to be stem primates (Bloch et al. 2007; Silcox 2008; Silcox et al. 2017) while others pace them as being more closely related to dermopterans, commonly known as flying lemurs (Beard 1990, 1991; Kay et al. 1990; Kay et al. 1992). Plesiadapiforms first appear in the earliest Paleocene (Pu 1, the first subdivision of the Puercan North American

Land Mammal Age) (Wilson et al. 2021), but quickly diversify into a morphologically and ecologically diverse group of mammals that includes 11 families known from North America, Europe, and Asia (Silcox et al. 2017). Of the eleven families of plesiadapiforms, nine have first appearance dates (FADs) in the Paleocene, only five of which successfully traverse the Paleocene–Eocene boundary. Plesiadapiform diversity generally wanes during the Eocene (Silcox et al. 2017). Many researchers hypothesize this slow decline in plesiadapiform diversity may reflect competition with euprimates, which first appear in the fossil record of North America during the earliest Eocene (Rose 1981; Gunnell 1986; Prufrock et al. 2016).

In terms of their spatial distribution and temporal duration, paromomyids are one of the most successful families of plesiadapiforms. Paromomyids first appear in the early Paleocene (Torrejonian 1) (Clemens and Wilson 2009) and persist until the early late Eocene (early Chadronian) (Kihm and Tornow 2014). This family currently includes seven genera: *Paromomys, Phenacolemur, Ignacius, Acidomomys, Arcius, Elwynella,* and *Edworthia.* This is the only plesiadapiform family that is known to be distributed across the three Holarctic continents of North America, Europe, and Asia and the only family that is known to occur above the Arctic Circle (Eberle and Greenwood 2012; Silcox et al. 2017). Although Asian paromomyids have been mentioned in the literature, they have not yet been formally described (Tong and Wang 1998; Silcox et al. 2017).

Within Paromomyidae, the genus *Ignacius* is of particular interest because it is one of two paromomyid genera known to range across the PETM (Bloch et al. 2007; Bown and Rose 1976). *Ignacius* is also the longest lived genus within the family, being first documented from the middle Torrejonian North American Land Mammal Age (NALMA) (Scott et al. 2013) and remaining fairly common throughout the Paleocene. While *Ignacius* traverses the

Paleocene/Eocene boundary, it mirrors the pattern of other plesiadapiforms and decreases in abundance during the early Eocene. An unknown species of *Ignacius*, known from a single tooth, has been recovered from the early Chadronian (late Eocene) (Kihm and Tornow 2014). If this specimen has been correctly identified as *Ignacius,* it would imply an approximately 13-million-year ghost lineage for the genus.

While the family Paromomyidae is temporally the most persistent, it is also the most geographically diverse, and the genus *Ignacius* provides the northern and southernmost occurrences of paromomyids in North America from Texas to the Canadian Arctic (Schiebout 1974; Eberle and Greenwood 2012). Also unique is that *Ignacius* is the only genus of plesiadapiform, and only member of Euarchonta, to occur above the Arctic Circle.

In the mid 1970's, vertebrate paleontologist Mary Dawson led pioneering field work in search of fossil vertebrates in the Canadian Arctic Archipelago on Ellesmere, Axel Heiberg, Devon, Ellef, Ringnes, Bylot, and Banks Islands (Eberle and McKenna 2007) (Figure 1). During the eleven field seasons conducted by Dawson and her team, fossil vertebrates dating to the Eocene Epoch were found on both Ellesmere and Axel Heiberg Islands, Canada's easternmost Arctic islands (Eberle and McKenna 2007). By far, the most diverse vertebrate faunal assemblages were found on central Ellesmere Island in two distinct faunal levels of the Margaret Formation (West and Dawson 1978; Dawson 1990; Eberle 2005; Eberle and Greenwood 2012; Eberle and Eberth 2015). The lower faunal level on central Ellesmere Island has produced a wide diversity of vertebrate taxa, including fish, reptiles, and at least 25 genera of mammals (Eberle and Greenwood 2012). The upper faunal level of the Margaret Formation does not match the lower level in terms of faunal diversity, but has produced two genera of mammals and a handful of non-marine, non-mammalian vertebrates (Eberle and Greenwood 2012).

The recovered mammalian fauna from the Margaret Formation shares remarkable similarities with faunas from Wasatchian-aged localities at mid-latitudes of North America. Eberle and Greenwood (2012) estimate that approximately two-thirds of the mammalian genera present on Ellesmere Island, including *Coryphodon, Viverravus, Homogalax, Ignacius* and others, are also present at contemporaneous mid-latitude localities. While the Eocene Arctic shares many similarities with mid-latitude faunas, there are some interesting differences. The family Plagiomenidae is fairly common and diverse in the Arctic assemblage but rare at mid-latitudes during the Wasatchian (Eberle and Greenwood 2012). Conversely, taxa like *Hyracotherium* and the hyopsodontid 'condylarth' *Hyopsodus* are incredibly abundant at mid-latitudes but absent in the Arctic assemblage (Eberle and Greenwood 2012). There is also a conspicuous absence of artiodactyls in the mammalian fauna from Ellesmere, even though they are relatively common at mid-latitude localities and despite the fact that artiodactyls are the only modern ungulates populating Arctic ecosystems today (Eberle and Greenwood 2012).

The similarities between the Arctic fauna of Ellesmere Island and mammalian assemblages in mid-latitude North America, suggest a late Wasatchian age for the vertebrate-bearing strata of the Margaret Formation (Eberle and Greenwood 2012). Paleoclimatology estimates suggest the Eocene of Arctic Canada would have represented a warm-temperate ecosystem comparable to modern day cypress swamps of the American southeast, with winter temperatures at or just above freezing (Francis 1988; Eberle 2005; Eberle and Greenwood 2012; West et al. 2015; West et al. 2020). The Eocene greenhouse produced a unique ecosystem where a warm, humid environment occurred in tandem with the near six-month light cycles of the Arctic (Eberle and Greenwood 2012). This raises questions about how the Eocene flora and fauna adapted to accommodate nearly six months of darkness during temperate, Arctic winters.

Although the two new species of paromomyids from Ellesmere Island were tentatively referred by the late Malcolm McKenna to the genus *Ignacius*, they have so far escaped official description even though the specimens were collected by Dawson and her team in the mid-late 1970's. Here, I will describe and diagnose the two new species of *Ignacius* as well as conduct a phylogenetic analysis to reconstruct their position on the paromomyid family tree. The results of the phylogenetic reconstruction will inform hypotheses regarding the historical biogeography of these unique mammals. Specifically, the phylogenetic analysis will provide a basis to test whether the Ellesmere paromomyids dispersed to the Arctic from mid-latitudes of North America, or whether they diverged from the European paromomyid, *Arcius*, and dispersed to the Arctic via the North Atlantic Land Bridge that connected Greenland to northwestern Europe during the earliest Eocene (Eberle and Greenwood 2012; López-Torres and Silcox 2018).

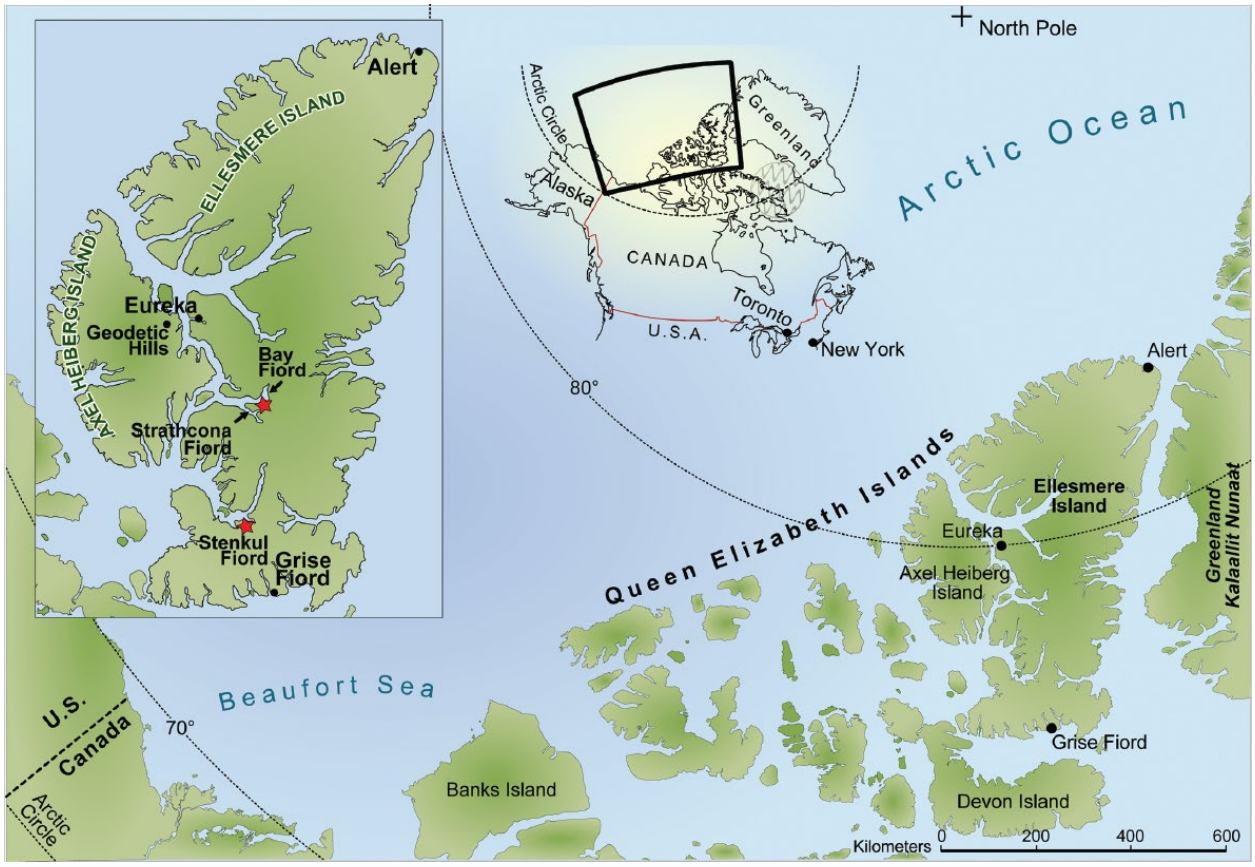

Figure 1: Map of the Canadian Arctic Archipelago. Red stars indicate location of prominent fossil vertebrate bearing localities of the lower faunal level on Ellesmere Island at Bay Fiord and Stenkul Fiord. Figure from Eberle and Greenwood (2012).

Paromomyidae: Previous Work

The family Paromomyidae has had a complicated taxonomic history. The first genus of paromomyid, *Phenacolemur*, was described by W. D. Matthew and Walter Granger in 1915 although it was originally placed within the family Apatemyidae in the order Insectivora (Matthew and Granger 1915). Twenty-five years later Simpson (1940) established Paromomyinae as a subfamily within Anaptomorphidae. The family rank Paromomyidae would not be officially used for another twenty-five years until Van Valen and Sloan (1965) elevated paromomyids from the subfamily to the family level. Four genera were included in Simpson's subfamily classification: *Paromomys, Palaechthon, Palenoctha,* and *Plesiolestes.* The inclusion of these genera in Paromomyinae was based on multiple dental characteristics including

procumbent incisors with a long, posteriorly extending root, simple p4s (see Chapter 3 Materials and Methods and Figure 4 for dental terminology), lower molars with mesiodistally compressed but wide trigonids, and upper molars without hypocones but an extended distolingual basin (Simpson 1940). *Palaechthon, Palenochtha*, and *Plesiolestes* have since been designation to separate families and are no longer considered to be paromomyids.

In 1955, Simpson proposed a new family, Phenacolemuridae, which he placed in the order Primates (Simpson 1955). This family included the genera *Phenacolemur, Paromomys*, and *Palaechthon*. This family was based on a myriad of dental characteristics, many of which mirrored the diagnostic characters of his proposed subfamily Paromomyinae. Some of the additional characteristics include: the loss of p1, reduced or absent p2-3, broad talonid basins, a prominent hypoconulid lobe with a double hypoconulid on m3, a reduced P3, and well developed submolariform P4 with a prominent protocone (Simpson 1955).

The type genus *Paromomys* is the only genus of the original four to still be included in what is currently considered Paromomyidae. Current definitions of Paromomyidae began with Bown and Rose (1976) where they included only three genera, *Ignacius, Phenacolemur,* and *Paromomys*, within the family. Low crowned molars with blunt cusps, lower molars with low, anteriorly inclined trigonids, reduced or absent paraconids, and upper molars with strong paracones and weak or absent conules joined the list of diagnostic characters started by Simpson in 1940 (Bown and Rose 1976). In the decades following Bown and Rose's (1976) revision, newly discovered specimens have been described and attributed to Paromomyidae such as: *Elwynella* (Rose and Bown 1982), *Arcius* (Godinot 1984), *Acidomomys* (Bloch et al. 2002), and *Edworthia* (Fox et al. 2010).

The genus *Ignacius* was originally described by Matthew and Granger (1921). *Ignacius* was originally included in the family Plesiadapidae which, at the time, was placed within the order Insectivora (Matthew and Granger 1921). The first *Ignacius* specimens were collected from the Mason Pocket locality in Colorado dating to the Tiffanian NALMA (Matthew and Granger 1921). The genus was named for the town of Ignacio, Colorado near the type locality (Matthew and Granger 1921). The type species for this genus is *Ignacius frugivorus* and was described from a maxillary fragment with a canine and P4-M2 along with the alveoli for the missing cheek teeth (Matthew and Granger 1921). The generic characters included in the original description include: a small, double rooted upper canine, a nearly molariform P4 with a small metacone compared to paracone and no crests connecting the paracone and metacone. What was originally described as a double-rooted upper canine is now agreed to be a P2 (Simpson 1935). Upper molar characters included buccal cusps that are subequal in size, absence of conules, a broad, sloping posterolingual angle, and low pre/postprotocristae. In 1955, Simpson concluded that *Ignacius* was a junior synonym to *Phenacolemur.* Subsequently, Robinson (1968) named *Ignacius* as a subgenus within *Phenacolemur*. Finally, in 1976, Bown and Rose revived *Ignacius* as a genus with an emended diagnosis differentiating it from *Phenacolemur* based on the following characteristics: smaller p4 compared to m1, shallow basins on upper and lower molars, and strongly oblique postproto/premetacristae (Bown and Rose 1976). There are currently four species within this genus: *I. frugivorus, I. fremontensis, I. graybullianus,* and *I. clarkforkensis.*

The first species of *Ignacius* that was described in 1921 by Matthew and Granger was *Ignacius frugivorus* (Matthew and Granger 1921). This species from the Tiffanian was based on three specimens with the following diagnostic characters: no paraconid on lower molars, subequal protoconid and metaconid, and a broad basined talonid lacking a hypoconulid

(Matthew and Granger 1921). Upper molar diagnostic characteristics are the same as the generic characteristics presented by Matthew and Granger (1921). *I. frugivorus* was referred to as *Phenacolemur frugivorus* beginning in 1955 with Simpson's publication, until Bown and Rose (1976) revived *Ignacius* as a genus level classification.

A second species of *Ignacius* would not be described for another fifty years, although it would be described as *Phenacolemur fremontensis* (Gazin 1971) and reclassified as *Ignacius* by Bown and Rose (1976). This is the oldest known species of *Ignacius* and is found as early as the late Torrejonian (Scott 2003). The first specimens of this species described by Gazin (1971) were collected in the Shotgun Member of the Fort Union Formation of the Wind River Basin, Wyoming. The type specimen for this species is a lower jaw fragment with p4-m1 and the original series consisted of an additional twelve isolated molars (Gazin 1971). This species is described as having an enlarged posterolingual basin and mostly differs from *I. frugivorus* in having slightly different p4 to m1 proportions (Gazin 1971).

Bown and Rose (1976) described the largest species of *Ignacius* at the time, *I. graybullianus*. This species was first collected from the early Eocene Willwood Formation, Wyoming and dates to the Wasatchian (Bown & Rose 1976). Apart from an overall increase in size, this species differs from the previously described species in having more squared upper P4s and more obliquely oriented postparacone/premetacone cristae (Bown and Rose 1976).

In 1968, Robinson described the species *Phenacolemur mcgrewi,* a species within the subgenus *Ignacius* (Robinson 1968). There has been some debate over the placement of this taxon and Bown and Rose (1976) refer to this taxon as *Ignacius mcgrewi,* disagreeing with Robinson's (1968) subgenus classification. Krishtalka (1978), however, continued to place this taxon in the genus *Phenacolemur*. Most recently, Lopez -Torres et al. (2018) re-designated this

taxon to the new genus *Walshina* in the family Omomyidae, a family within Euprimates. This species was found in the late Eocene (Uintan NALMA) Bad Water Creek localities of Wyoming (Robinson 1968). The placement of this taxon within Paromomyidae would result in this specimen being the youngest known member of the family (López-Torres et al. 2018). Morphologically, paromomyids closely resemble omomyids, especially the genus *Trogolemur*, but occur most commonly in the Paleocene and early Eocene (López-Torres et al. 2018). According to López-Torres et al. (2018) lower molars with strong paracristids and hypoconulids, strong, oblique postvallid in m1, well developed hypoconulids on lower molars, and differing degrees of expansion of the distolingual basin all indicate that the originally described *Phenacolemur mcgrewi* belongs to the family Omomyidae, specifically the tribe Trogolemurini.

The most recent species to be classified to the genus *Ignacius* is *I. clarkforkensis,* described by Bloch et al. (2007). This species dates to the latest Paleocene (Clarkforkian NALMA) of the Clark Forks Basin, Wyoming, occurring temporally intermediate to the middle Paleocene *I. fremontensis* (Gazin 1971) and *I. frugivorus* (Matthew & Granger 1921) and the early Eocene *I. graybullianus (*Bown & Rose 1976). This species is larger than *I. graybullianus* and differs from the other species in having a single-rooted P2 (Bloch et al. 2007). *I. clarkforkensis* is similar to *I. graybullianus* in having more obliquely-oriented postpara/premetacristae on upper molars when compared to the two earlier occuring species (Bloch et al. 2007). *I. clarkforkensis* further differs from other species in having different molar dimension ratios (Bloch et at. 2007).

Paromomyid fossil material is represented by cranial, dental, and postcranial specimens. While plesiadapiforms are, in general, known to be arboreal, the group show a wide array of arboreal adaptations and the skeletal morphology of paromomyids suggest they were adapted to

vertical clinging and climbing on large diameter supports (Bloch et al. 2007). Similar arboreal behavior has been seen in the extant callitrichine primates and is associated with feeding on plant exudates (Garber 1992). This has led researchers to hypothesize that paromomyids filled a similar ecological niche to extant small bodies mammals known to feed on exudates (Beard 1991; 1993; Bloch et al. 2007).

Table 1: Comparison of average dental measurements (mm) of known species of *Ignacius*

Species	*Species 1*	*Species 2*	*I. graybullianus**	*I. clarkforkensis* †	*I. frugivorus* ł	*I. fremontensis* §
P4 Width	-	-	2.30	2.60	2.14	-
P4 Length	-	-	1.85	1.99	1.69	-
M1 Width	5.14	3.91	2.90	3.23	2.91	-
M1 Length	4.11	3.19	2.15	2.66	1.97	-
M2 Width	-	3.86	2.75	3.12	2.93	2.50
M2 Length	-	3.80	2.00	2.35	1.89	1.60
M3 Width	-	3.08	2.70	2.94	2.08	-
M3 Length	-	4.21	2.15	2.18	1.30	-
p4 Width	-	2.09	1.75	1.66	1.34	0.90
p4 Length	-	2.26	1.75	2.17	1.96	1.30
m1 Width	3.52	3.06	2.00	2.22	1.74	1.20
m1 Length	4.26	3.41	2.15	2.58	2.04	1.70
m2 Width	4.00	2.90	2.05	2.20	1.76	1.30
m2 Length	4.68	3.30	2.05	2.57	2.15	1.70
m3 Width	-	3.19	1.85	2.04	1.52	1.20
m3 Length	-	5.07	3.20	3.43	2.77	2.30

*Measurements from Bown and Rose 1976
† measurements from Bloch et al. 2007
ł measurements from Secord 2008
§ measurements from Gazin 1971

2. Geologic Setting

Ellesmere Island and the surrounding islands of the Canadian Arctic Archipelago in Nunavut host a series of formations that are contained within the Eureka Sound Group, which date from the Late Cretaceous through the mid-late Eocene (Eberle and Greenwood 2012). The Eureka Sound Group has had a complicated history of classification. This stratigraphic unit was originally described as a group by Troelson (1950), but subsequently lowered to the level of formation by Tozer (1963). Finally, in 1986, the Eureka Sound unit was again raised to the group level by Miall (1986), where it has since remained. Throughout its history, the terrestrial vertebrate-bearing strata near Bay Fiord on central Ellesmere Island have been mapped by multiple researchers, resulting in three separate names referring to the same stratigraphic section - member IV of West et al. (1981), the Iceberg Bay Formation of Ricketts (1986), and the Margaret Formation of Miall (1986). Today, the Eureka Sound Group is commonly subdivided into four formations, with Miall's (1986) terminology most often applied to Ellesmere and Banks Islands, and Ricketts's (1986) formational subdivisions used on nearby Axel Heiberg Island (Eberle and Greenwood, 2012; Eberle and Eberth 2015).

The Eocene localities on Ellesmere Island that produce non-marine, terrestrial vertebrates occur within the Margaret Formation (Eberle and Eberth 2015). The Margaret Formation consists of coarsening upwards cycles of interbedded cross-bedded sandstone, siltstone, mudstone, and coal (Eberle and Eberth 2015) (Figure 2). These observations are interpreted to represent proximal delta-front to delta-plain paleoenvironments characterized by lowland swamps and channels (Miall 1986; Eberle 2005). Terrestrial vertebrates have been found at two distinct stratigraphic levels within the Margaret Formation near Bay Fiord (Eberle and Greenwood 2012), which are separated by a 478 meter thick stratigraphic gap that appears to

lack fossil vertebrates (Eberle and Eberth 2015).The lower faunal level has yielded a diversity of fish, reptiles, and at least 25 genera of mammals. This faunal assemblage has been correlated with the late Wasatchian NALMA (late-early Eocene), based on similarities in faunal composition to vertebrate localities in mid-latitude North America during this interval (Eberle and Eberth 2015). The presence of Wasatchian index taxon *Pachyaena* on Ellesmere Island, as well as taxa like *Heptodon, Eotitanops,* and *Miacis*, all of which first appear during the Wasatchian at mid-latitude localities in North America, corroborate a late Wasatchian age for the lower faunal level of the Margaret Formation (Eberle and Greenwood 2012). Zircon crystals recovered from a volcanic ash near Stenkul Fiord, on southern Ellesmere Island, have been dated to 53.7 +/- 0.6 Ma, suggesting a middle Wasatchian age for the Stenkul Fiord vertebrate localities, which are slightly higher in the section than the dated volcanic ash layer (Reinhardt et al. 2017; Von Gosen et al. 2019). Based on biostratigraphy and the stratigraphic proximity of the Stenkul Fiord vertebrate localities and the volcanic ash layer, the Stenkul Fiord localities appear to be slightly older than the late Wasatchian localities from Bay Fiord (Eberle and Eberth 2015).

The upper faunal level known from the Margaret Formation at Bay Fiord is thought to date to the middle Eocene Bridgerian NALMA. This faunal level contains a very limited number of recovered taxa when compared with the diverse assemblage found in the lower faunal zone, with only two known mammalian taxa (Eberle and Greenwood 2012). The mammalian taxa recovered from the upper faunal level include the brontothere *Palaeosyops*, a larger brontothere taxon than is found in the lower faunal level (Eberle and Eberth 2015), and a tooth fragment tentatively identified as a stylinodontid taeniodont (Eberle and Greenwood 2012). Several nonmammalian, nonmarine vertebrates have also been found from the upper faunal level, most notably, an anosteirine turtle, which has an earliest occurrence in the early Bridgerian at mid

latitudes in North America (Eberle and Greenwood 2012). The occurrence of the brontothere *Palaeosyops*, which is a more advanced taxon than seen in the lower faunal level, along with the presence of the anosteirine turtle, suggest an early Bridgerian age for the upper faunal level (Eberle and Greenwood 2012).

The paromomyid plesiadapiform specimens that are the focus of this study were recovered from five localities within the late Wasatchian-aged lower faunal level near Bay Fiord on central Ellesmere Island. Of the 32 paromomyid specimens, 23 were recovered from locality ELS (Ellesmere) 76-85 (coined Locality 85 in earlier publications), six were recovered from locality ELS 76-44, and only one specimen each was recovered from the remaining localities, ELS 76-49, ELS 76-56, and ELS 76-84. Three of the paromomyid-bearing localities, ELS 76-85, 76-49, and 76-44, have been tied into the stratigraphic section of Eberle & Eberth (2015) (Figure 3), placing many of the localities near Bay Fiord sequentially within the stratigraphic framework of the lower faunal level. While all of these localities are considered late Wasatchian, of the three localities tied to the stratigraphic section, locality ELS 76-49 seems to be the lowest in the section at ~1305 m, whereas the very productive ELS 76-85 locality is the highest at 1437 m (Eberle and Eberth 2015). Stratigraphically, locality ELS 76-44 is intermediate between the other two localities at 1405 m (Figure 3) (Eberle and Eberth 2015).

Figure 2: Geologic exposures of the Margaret Formation near Bay Fiord on central Ellesmere Island. Image taken in 2010 by Jaelyn Eberle.

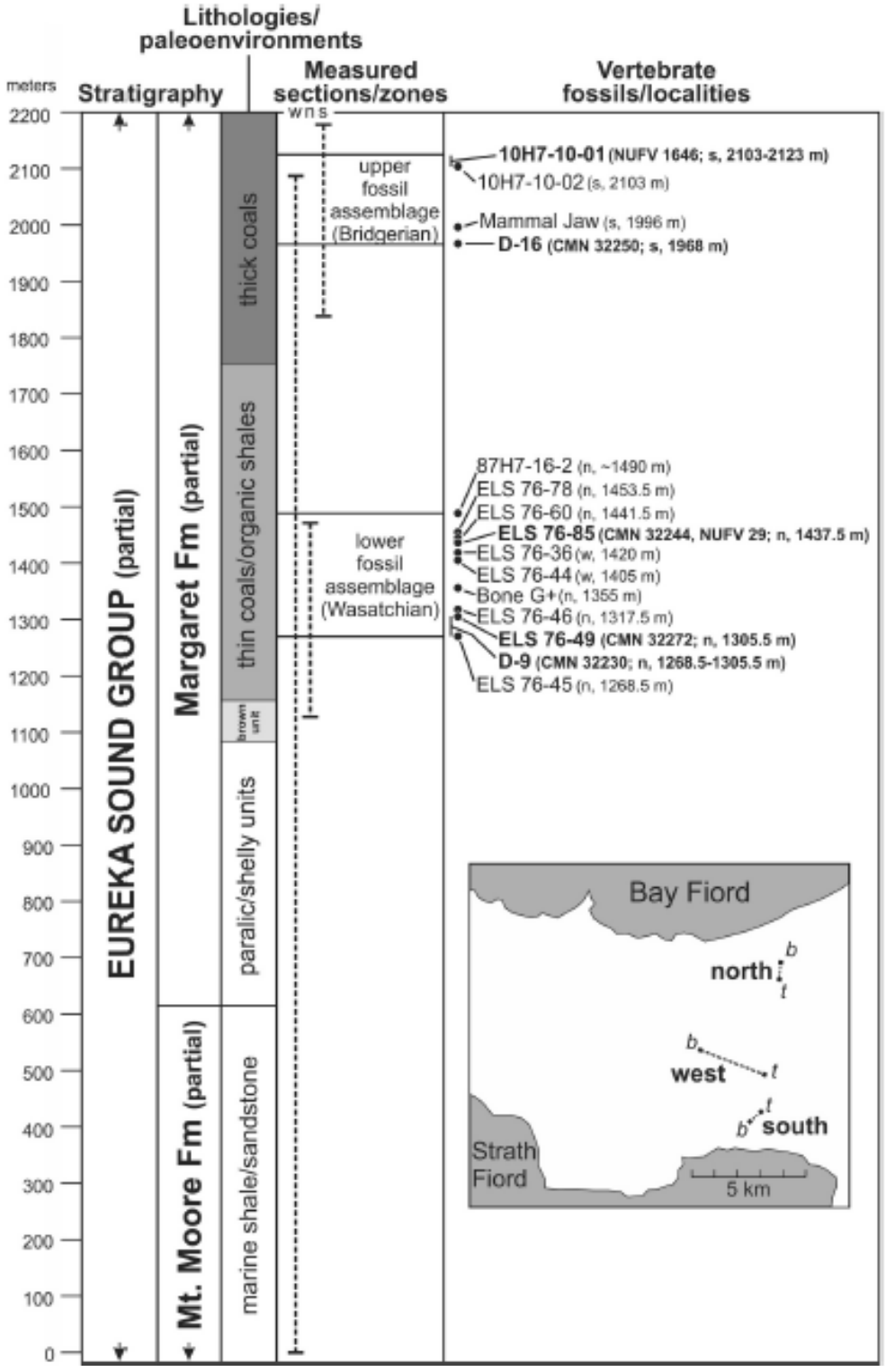

Figure 3: Composite litho- and biostratigraphy of fossil localities at Bay Fiord including three prominent localities that produced new paromomyid material, 76-85, 76-44, and 76-49, from the lower faunal level of the Margaret Formation. From Eberle and Eberth 2015.

3. Materials and Methods

The fossil specimens described in this analysis are from the Canadian Museum of Nature and on loan to the University of Kansas Natural History Museum. The new paromomyid specimens were compared with specimens from the University of Kansas Division of Vertebrate Paleontology, specimens on loan from the University of Colorado Museum of Natural History, and cast specimens from the American Museum of Natural History, Princeton University, University of Alberta Laboratory of Vertebrate Paleontology, University of Michigan Museum of Paleontology, Yale Peabody Museum, Université de Montpellier, as well as images and descriptions from the literature.

Dental measurements for the new paromomyid specimens were obtained using a Unitron Z series binocular microscope equipped with Mitutoyo digimatic micrometers, using the methodology of Bloch and Gingerich (1998) (Figure 4). Dental metrics for *I. graybullianus, I. clarkforkensis, I. frugivorus,* and *I. fremontensis* were obtained from previously published literature (Gazin 1971; Bown and Rose 1976; Bloch et al. 2007; Secord 2008).

The new paromomyid specimens were scanned via micro computed tomography (micro-CT) at the Museo Nacional de Ciencias Naturales. 3D meshes of *I. graybullianus, I. clarkforkensis, I. frugivorus, I. fremontensis, Paromomys farrandi, Phenacolemur archus,* and *Arcius rougieri* used to generate comparative figures were downloaded from Morphosource. All 3D data were rendered using Autodesk 3ds Max 2021.

The phylogenetic analysis was performed using PAUP* 4.0a (Swofford 2002). Detailed methodology for the phylogenetic analysis is presented below in Chapter IV, Systematic Paleontology.

Institutional Abbreviations and Repositories

AMNH, American Museum of Natural History, New York, New York: **CMN**, Canadian Museum of Nature, Ottawa, Ontario, Canada; **KUVP**, Division of Vertebrate Paleontology, Biodiversity Institute, University of Kansas, Lawrence, Kansas; **MNCM**, Museo Nacional de Ciencias Naturales, Madrid, Spain; **PAT**, Université de Montpellier (Palette collection), Montpellier, France; **PU**, Princeton University, Princeton, New Jersey; **UALVP**, University of Alberta Laboratory of Vertebrate Paleontology, Edmonton, Alberta, Canada; **UCM**, University of Colorado Museum of Natural History, Boulder, Colorado; **UM**, University of Michigan, Ann Arbor, Michigan; **YP,** Yale Peabody Museum, New Haven, Connecticut.

Dental Terminology

I/I, Upper/lower incisor; **P/p**, Upper/lower premolar; **M/m**, Upper/lower molar.

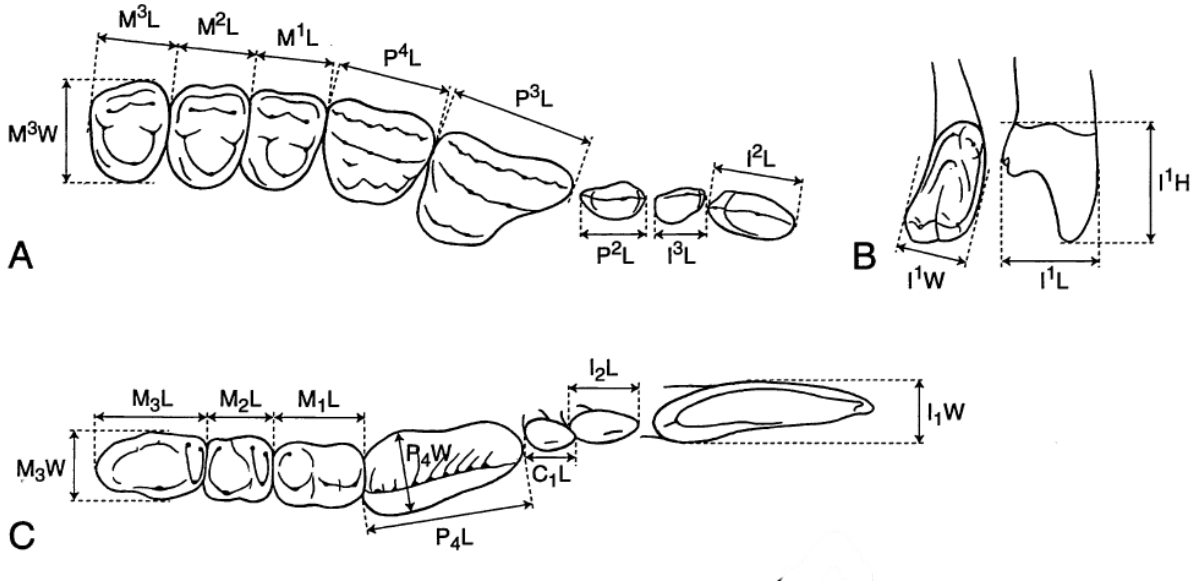

Figure 4: Summary of dental measurements. **A**, upper cheek teeth. **B**, upper incisors. **C**, lower dentition. Adapted from Bloch and Gingerich 1998.

4. Systematic Paleontology

Class Mammalia Linnaeus, 1758

Cohort Placentalia Owen, 1837

Mirorder Primatomorpha Beard, 1991

Suborder Plesiadapiformes Simons and Tattersall, 1972

Family Paromomyidae Simpson, 1940

Genus *Ignacius* Matthew and Granger, 1921

Type Species—*Ignacius frugivorus* Matthew and Granger, 1921.

Etymology— Named for the town of Ignacio, Colorado near the type locality, Mason's Pocket.

Included Species—*Ignacius frugivorus* Matthew and Granger, 1921; *Ignacius fremontensis* Gazin, 1971; *Ignacius graybullianus* Bown and Rose, 1976; *Ignacius clarkforkensis* Bloch et al., 2007.

Occurrence—Middle Paleocene (middle Torrejonian) through early Eocene (Wasatchian) of North America.

Ignacius sp. 1, sp. nov.

Holotype—CMN 30830, left maxillary fragment with M1 and the alveoli for P4 and M2.

Hypodigm—The holotype; CMN 30986, left dentary fragment with roots of i1 and p4 and crown of m1; CMN 30850, left dentary fragment with the alveolus of i1, roots of p4-m1, and crown of m2.

Etymology—To be determined.

Type Locality—Ellesmere Island (ELS) locality 76-85, lower faunal level of the Margaret Formation, Eureka Sound Group, Ellesmere Island, Nunavut, Canada (Wasatchian).

Known Distribution—The type locality and 76-56, lower faunal level of the Margaret Formation, Eureka Sound Group, Ellesmere Island, Nunavut, Canada.

Diagnosis—Largest known species of *Ignacius.* Differs from other species of *Ignacius* in having crenulated molar enamel and broad buccal cingula on upper molars. M1 with neomorphic crest or preprotocingulum linking protocone with mesiolingual cingulum. Postprotocrista on M1 relatively weak, so that trigon and posterolingual basins are nearly continuous. M1 buccolingually compressed resulting in a more square occlusal outline than in either *I. fremontensis* or *I. frugivorus*. Origin of zygomatic arch more anterior than seen in other species of *Ignacius* except *I. graybullianus*. Lower m1-2 with distinct buccal cingula on talonids. Molar crown area of Species 1 approximately four times larger than *I. clarkforkensis*.

Description

Maxilla— The CMN 30930 maxillary fragment is the only maxilla in this assemblage. The root of the zygomatic arch is positioned anteriorly and originates just anterior to the M1. The infraorbital foramen seems to be positioned directly superior to the mesiobuccal alveolus of P4. When viewing this maxilla in buccal view, the anterior portion of the maxilla arcs inferiorly (Figure 5).

M1—The M1 is buccolingually compressed, resulting in a more nearly square occlusal outline than occurs in the upper molars of other *Ignacius* species, particularly *I. fremontensis* and *I. frugivorus* which have comparatively short molars mesiodistally and wide molars buccolingually. The paracone and metacone are almost equal in height, with the metacone being only slightly shorter than the paracone. A strong buccal cingulum is present, which becomes

continuous with the postmetacrista at the distobuccal margin of the tooth. A short, weakly defined preparacrista is present. The postparacrista and premetacrista are not as obliquely oriented as in *I. clarkforkensis* or *I. graybullianus* but more oblique than in *I. frugivorus* and *I. fremontensis*. The postprotocrista is present but relatively weak, so that the trigon and posterolingual basins are nearly continuous. A neomorphic crest that is designated here as a preprotocingulum (Figure 5) runs mesially from the protocone, connecting the latter cusp with the precingulum. The preprotocrista runs mesiolingually from the protocone, becoming continuous with the mesial cingulum near the site where a weak crest that may be homologous with the postparaconule crista diverges toward the apex of the paracone. Distinctly cuspate paraconule and metaconule are absent, although minor swelling on the postprotocrista may mark the location of a vestigial metaconule. Cusps and crests are relatively blunt, especially the protocone. Because of the nearly square occlusal outline of M1, the postprotocingulum is relatively longer than it is in *I. fremontensis* and *I. frugivorus*. The trigon and posterolingual basins are shallow, nearly continuous, and both show enamel crenulation.

Dentary— Both CMN 30850 and CMN 30986 preserve portions of the dentary. Two mental foramina are present on the buccal side of each dentary but seen more clearly in CMN 30986. The anterior mental foramen is positioned directly inferior to the mesial p4 root and the posterior mental foramen is positioned inferior to the mesial m1 root. The roots of p4 are significantly splayed inferiorly but become relatively closely appressed near where the crown, if present, would begin. The distal p4 root seems to be buccolingually expanded when compared to the mesial p4 root so that it is almost equal in width to the mesial root of m1. A strong dorsal crest is present from the i1 alveolus to the lingual aspect of the mesial p4 alveolus.

m1–2 — While neither of the dentary specimens (CMN 30850 and CMN 30986) preserve the crown of p4, the distance between the p4 roots suggests a more mesiodistally compressed p4 than the p4 seen in *I. fremontensis* and *I. frugivorus* which are relatively long and narrow. Overall molar size is ~60% larger than in *Ignacius clarkforkensis*. The paraconid is less distinct and more closely appressed to the metaconid than seen in *I. fremontensis* and *I. frugivorus.* Additionally, the protoconid and metaconid are spaced further apart in this species resulting in a trigonid that is broader than seen in other *Ignacius* species. Lower molar cusps are blunt but the protoconid and hypoconid are especially indistinct. A small paraconid is present but closely appressed to the metaconid. The paracristid runs mesially from the protoconid with only a slight inferior slope. A buccal cingulid is present on the talonid of m1-2. The m2 paraconid is taller than the metaconid, although a longitudinal crack runs through the central part of the trigonid and talonid of this tooth. The cristid obliqua on m1 and m2 is less obliquely oriented than in other species of *Ignacius*. The m1 cristid obliqua meets the distal wall of the trigonid just lingual to the protoconid and the m2 cristid obliqua runs parallel to the buccal cingulid, meeting the postvallid at the base of the protoconid. In contrast to *I. fremontensis* and *I. frugivorus*, lower molar trigonids are low and talonid basins are broad and shallow. In these respects, the new Ellesmere species resembles *I. graybullianus* and *I. clarkforkensis.* Moderate crenulation is present in the lower molar talonid basins of the new species.

Table 2: Summary of dental measurements (mm) for Species 1 from Ellesmere Island, Nunavut, Canada

Tooth Locus	n	x	OR	s	V
M1 L	1	-	4.11	-	-
M1 W	1	-	5.14	-	-
m1 L	1	-	4.26	-	-
m1 W	1	-	3.52	-	-
m2 L	1	-	4.68	-	-
m2 W	1	-	4.00	-	-

Abbreviations: L, length; **W**, width; **n,** number of specimens; **x**, mean; **OR**, observed range; **s**, standard deviation; **V**, coefficient of variation

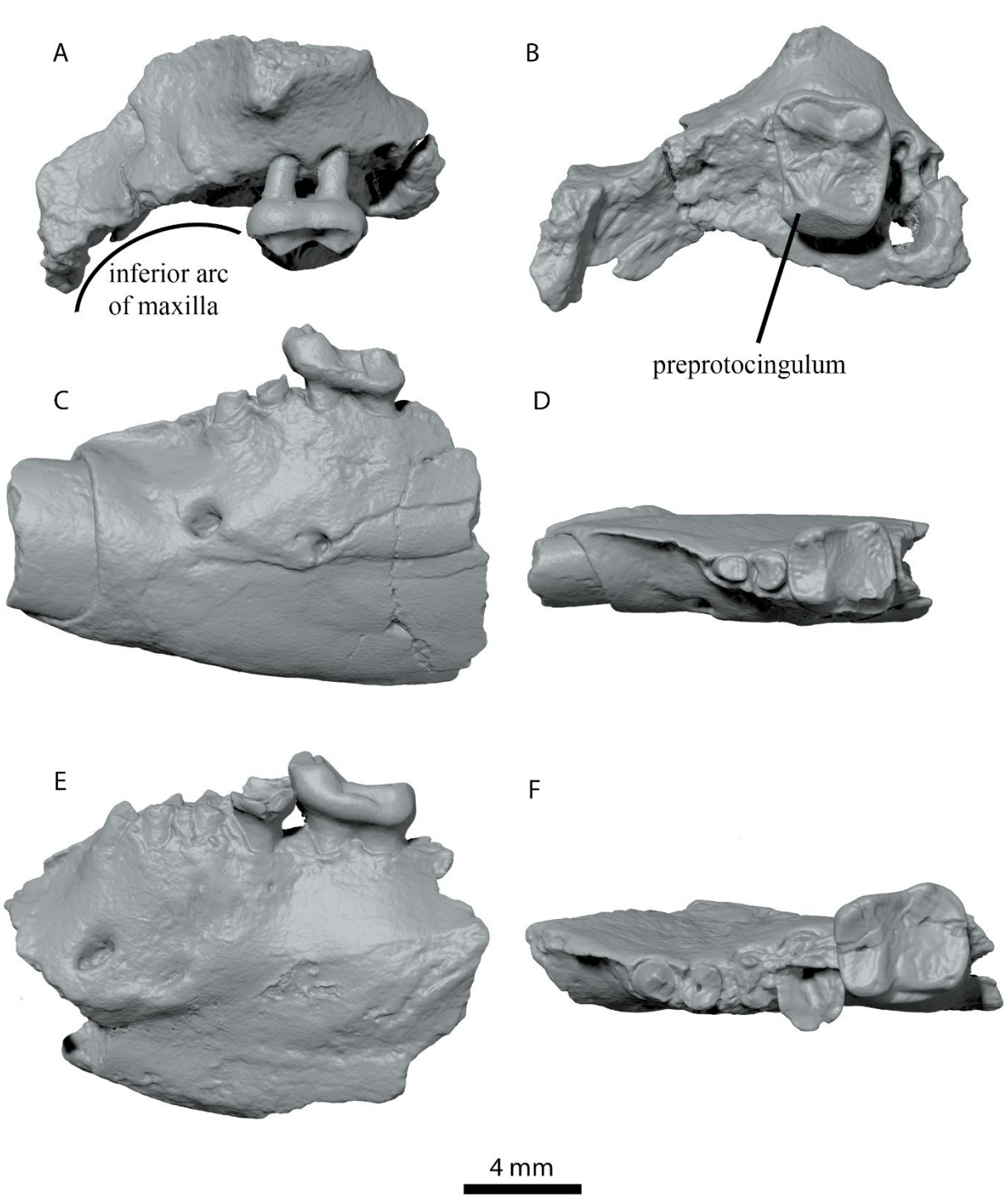

Figure 5: *Ignacius species 1*, sp. nov., dentary and maxilla fragments from the Eocene Margaret Formation, Ellesmere Island, Nunavut, Canada. Images rendered from Micro CT scans. **A-B,** CMN 30830, holotype left maxillary fragment preserving M1 and alveoli for P4 and M2 in **A,** buccal and **B,** occlusal views. **C-D,** CMN 30986, left dentary fragment preserving roots of i1 and p4 and crown of m1in **C**, buccal and **D,** occlusal views. **E-F,** CMN 30850, left dentary fragment preserving the alveolus for i1, the roots for p4-m1, and crown of m2 in **E,** buccal and **F,** occlusal views.

Ignacius sp. 2, sp. nov.

Holotype—Canadian Museum of Nature (CMN) 30868, left M2.

Hypodigm—The holotype; CMN 30828, right m1; CMN 30831, left dentary fragment preserving roots for m2 and talonid fragment of m3; CMN 30835, left edentulous dentary fragment preserving alveoli for p4-m2; (CMN) 30837, right dentary with p4-m1; CMN 30853, right edentulous dentary fragment preserving roots for i1-m1 and alveoli for m2-3; CMN 30856, right m2; CMN 30864, left m2; CMN 30867, fragmentary left m2; CMN 30883, fragmentary left m3; CMN 30889, left m3; CMN 30902, fragmentary right m3; CMN 30903, apical part of left I1; CMN 30927, right m3 talonid fragment; CMN 30933, fragmentary left m3; CMN 30936, left p4; CMN 30949, left p4; CMN 30954, left m1; CMN 30959, right m1; CMN 30988, left dentary fragment preserving roots of m2 and talonid of m3; CMN 30995, right M1; CMN 30996, right M2; CMN 30997, left m3; CMN 30998, right M2; CMN 30999, left m1; CMN 32320, right M1; CMN 32321, left M3; CMN 32325, fragmentary right I1.

Etymology— To be determined.

Type Locality—Ellesmere Island locality 76-85, lower faunal level of the Margaret Formation, Eureka Sound Group, Ellesmere Island, Nunavut, Canada (Wasatchian).

Known Distribution— The type locality, ELS localities 76-44, 76-49, 76-56, and 76-84, lower faunal level of the Margaret Formation, Eureka Sound Group, Ellesmere Island, Nunavut, Canada.

Diagnosis—Differs from other species of *Ignacius* in having upper molars with lower, less cuspate paracone and metacone more nearly integrated within the relatively straight, trenchant centrocrista. Differs from other species of *Ignacius* except *Ignacius* sp. 1 in having upper molars with well-defined preprotocingulum and crenulated enamel. Differs from *Ignacius*

sp. 1 in being ~40% smaller and having stronger enamel crenulation. M3 talon more elongated than in other *Ignacius* species. Trigonid of p4 broader than in other species of *Ignacius*, with neomorphic lingual expansion of protoconid and associated postvallid crest. Lower molars differ from those of *Ignacius fremontensis* and *I. frugivorus* in having stronger buccal cingulids, broader trigonids, and paraconid and metaconid more closely connate. Differs from other species of *Ignacius* in having m3 with low trigonid and relatively flat talonid lacking distinct cusps.

Description

I1—Two upper central incisors of *Ignacius* sp. 2 are known from two specimens. CMN 30903 is a relatively complete left I1, while CMN 32325 preserves the apical part of a right I1. Both specimens show an unusual wear pattern, in which the apices of the anterocone and laterocone are relatively pristine, while the mesiolingual surface of the crown below the anterocone and mediocone is heavily worn (Figure 6E). I1 is dominated by the anterocone and laterocone, which are labiolingually compressed cusps with sharp crests extending mesially and distally from their apices. A deep, V-shaped cleft divides the bases of the anterocone and laterocone. The apex of the laterocone projects distally away from the anterocone and is positioned more apically than in other *Ignacius* species, KUVP 157225, *I. fremontensis* and UM 110963, *I. frugivorus*, Figure 53 H. and I. of Secord (2008). A small but relatively pyramidal mediocone is present near the mesial base of the anterocone. A mediocrista is present, but its degree of development and full lingual extent are impossible to determine because of the heavy lingual wear noted previously. A flat interstitial wear facet for the contralateral I1 is present near the mesial base of the mediocone. Heavy wear obscures the morphology of the posterocone, but it appears not to have been very voluminous.

M1—CMN 32320 is the best-preserved specimen of M1 for this species. Like sp. 1, the upper M1 of sp. 2 is buccal-lingually compressed resulting in teeth with square occlusal outlines. The metacone is significantly shorter than the paracone and the paracone is displaced slightly buccally compared to the metaconid, but the buccal displacement of the paracone is not as exaggerated as seen in the M2 of this species. The buccal displacement of the paracone results in a postparacrista and premetacrista that are not obliquely oriented as seen in *I. clarkforkensis* and *I. graybullianus,* but form a nearly straight crest from the paracone and metacone when observed in occlusal view. When these structures are viewed in lingual view, the premetacrista meets the postparacrista with a slight "v" shape. While sp. 1 has a weak postprotocrista, sp. 2 has lost the postprotocrista entirely, resulting in one continuous basin with strong enamel crenulation. While *Ignacius* molar basins are diagnostically shallow, this species seems to express the greatest reduction in upper molar basin depth and the M1 basin is only very slightly concave.

M2—CMN 30868 is the best-preserved specimen if M2 for this species. The metacone is significantly shorter than the paracone and the paracone is significantly buccally displaced compared to the metacone, a feature that is especially enhanced in this tooth locus, resulting in a buccal margin with a steep distal slope. The postparacrista and premetacrista are not obliquely oriented in relation to each other but instead form a continuous, steep crest parallel to the buccal edge of the tooth (Figure 6I), unlike the strong, oblique crests seen in the previously described *Ignacius* species. When these structures are viewed in lingual view, the premetacrista does not slope inferiorly and crate a 'v' shape where it meets the postparacrista. Instead the premetacrista is nearly absent and instead creates a plateau in the area of the metacone before it meets with the steep, postparacrista which has a steep anterior angle. As seen in M1, M2 has lost the postprotocrista entirely. The preprotoprecingulum of M2 is more defined than in M1, but not

quite as defined as seen in sp. 1. Upper molar basins of sp. 2 are not concave, but instead exhibit a very gradual slope from the higher mesial cusps and crests, to low structures on the distal side of the tooth.

M3—CMN 32321 is the only specimen currently known that documents M3 morphology. The most notable and derived aspect of M3 is the extreme reduction of its trigon cusps, none of which are distinctly cuspate. The paracone and metacone are greatly reduced and fully incorporated within a mesiodistally straight centrocrista, which forms a crest along the mesiobuccal side of the crown. The protocone is slightly more distinct than the paracone and metacone, but it too is integrated within a raised and mesiodistally extensive postprotocingulum. The latter structure is continuous with a raised distal cingulum, which arcs around the distobuccal margin of the tooth before essentially fusing with the centrocrista mesially. Because of the great length of the postprotocingulum, a mesiodistally expanded talon basin occupies roughly half the areal extent of the entire crown. The postprotocrista is absent, so that the trigon and talon are confluent, shallowly basined, and adorned with extremely crenulated enamel. A short preprotocrista merges with a raised mesial cingulum, which joins the centrocrista near the mesiobuccal corner of the tooth. In general, the M3 crown forms a shallowly concave and highly crenulated surface that is surrounded on all sides by raised crests or cingula. A short precingulum is restricted to the mesiolingual side of the crown, extending from the level of the protocone to the junction between the preprotocrista and the raised mesial cingulum. The lingual root of M3 is greatly expanded mesiodistally, running almost the entire length of the crown, matching the expansion of the postprotocingulum and talon basin (Figure 6L). In contrast, the two buccal roots are small, closely spaced or even partly fused, and restricted to the mesial part of the tooth.

p4—Several specimens document the morphology of p4, among which only minor variation occurs. The p4 crown is remarkably short and broad, and the two roots are very closely spaced if not partly fused. The protoconid is wide buccolingually, and its distal surface forms the vertically oriented postvallid. Weak crests occur on either side of the postvallid, which meet at the apex of the protoconid. The buccal postvallid crest is confluent with the mesiodistally short cristid obliqua. As a result, the buccal side of the crown continues uninterrupted from the trigonid to the talonid, leaving no space for a hypoflexid. The lingual postvallid crest and the lingual side of the protoconid bulge lingually, where a tiny swelling of enamel could be considered a presumptive metaconid (Figure 7G). The mesial side of the protoconid is smoothly rounded, with no development of a mesial protoconid crest or paracristid. The talonid is mesiodistally short but wide, like that of *I. graybullianus.* The entoconid is relatively tall and cuspidate, while the hypoconid is shorter and blunt. Minor enamel crenulation occurs on the postvallid and in the talonid basin.

m1–2—The trigonids of m1 and m2 are mesiodistally short and broad, with paraconid and metaconid closely connate and a low protoconid. On relatively unworn specimens such as CMN 30828 and CMN 30999, a low but distinct protocristid runs transversely across the back of the trigonid, connecting the protoconid and metaconid. Mesial to the protocristid and running more or less parallel to it lies a transverse valley or groove. The m2 protoconid is especially reduced and raised only slightly above the talonid cusps. The protoconid is lower than the metaconid and paraconid and is relatively blunt, with a paracristid that slopes gradually from the apex, as seen in *I. graybullianus*. The postvallids of both m1 and m2 are canted mesially, resulting in very low-crowned teeth. Overall, the shape of the trigonid basin is rectangular. A weak buccal cingulid is present on m1, beginning at the base of the protoconid and terminating

on the distal aspect of the hypoconid. The buccal cingulid is absent in m2. The cristid obliqua of m1 joins the postvallid slightly lingual to the protoconid, yielding a modest hypoflexid. On m2 the cristid obliqua joins the postvallid farther buccally, and the hypoflexid is very shallow as a result. The talonid is broad, shallowly excavated and heavily crenulated. The m1 hypoconid and entoconid are approximately equal in height, while the m2 entoconid is taller than the hypoconid.

m3—The m3 talonid basin is extremely shallow and is essentially a flat plane with heavy enamel crenulation. Mesial inclination of the trigonid is the most pronounced on this tooth. The entoconid is the most distinct cusp but is still reduced and barely raised above the edge of the tooth. The cristid obliqua runs parallel with the edge of the tooth just lingual to the buccal cingulid. The trigonid on m3 is low and mesiodistally compressed as seen in other species of *Ignacius.* The protoconid is reduced and essentially absent as is the paraconid. The protocristid and paracristid are quite flat and just barely raised to form a weak border around the trigonid. While other *Ignacius* species lack definition on m3, Sp. 2 has the least topographic relief but the most dramatic enamel crenulation. Specimens preserving the distal aspect of the m3 talonid seem to express a raised distal cingulum that received heavier wear than adjacent structures on the talonid.

Table 3: Summary of dental measurements (mm) for Species 2 from Ellesmere Island, Nunavut, Canada

Tooth Locus	n	x	OR	s	V
I1 L	2	2.29	2.07-2.52	0.32	13.95
I1 W	2	3.50	3.29-3.71	0.30	8.58
M1 L	3	3.19	3.11-3.30	0.10	3.10
M1 W	3	3.91	3.74-4.03	0.15	3.84
M2 L	2	3.80	3.32-4.28	0.68	17.89
M2 W	2	3.86	3.54-4.18	0.45	11.66
M3 L	1	-	4.21	-	-
M3 W	1	-	3.08	-	-
p4 L	3	2.26	2.20-2.36	0.08	3.54
p4 W	3	2.09	2.00-2.29	0.17	8.13
m1 L	5	3.43	3.04-3.65	0.26	7.58
m1 W	5	3.03	2.85-3.24	0.15	4.95
m2 L	2	3.30	2.93-3.67	0.52	15.76
m2 W	2	2.90	2.56-3.23	0.47	16.21
m3 L	2	5.07	5.00-5.14	0.09	1.78
m3 W	6	3.19	3.09-3.37	0.11	3.45

Abbreviations: L, length; **W**, width; **n,** number of specimens; **x**, mean; **OR**, observed range; **s**, standard deviation; **V**, coefficient of variation

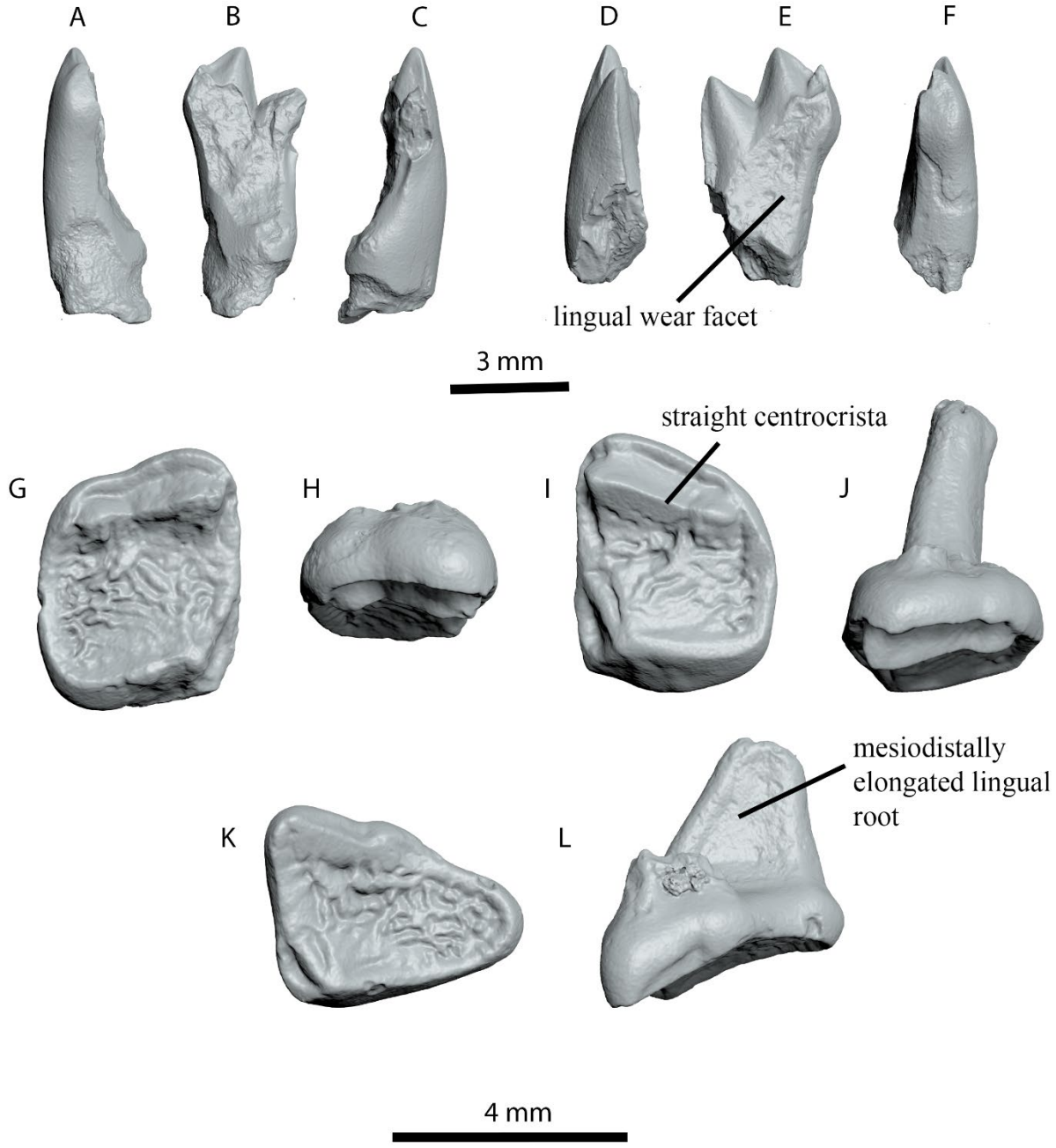

Figure 6: *Ignacius species 2* sp. nov., isolated upper teeth from the Eocene Margaret Formation, Ellesmere Island, Nunavut, Canada. Images rendered from Micro CT scans. **A-C,** CMN 30903, left I1, in **A**, mesial, **B**, lingual, and **C**, distal views; **D-F**, CMN 32325, apical fragment of right I1 in **D**, distal, **E**, lingual, and **F**, mesial views; **G-H**, CMN 32320, left M1 in **G**, occlusal and **H**, buccal views; **I-J**, CMN 30868, holotype, left M2 in **I**, occlusal and **J**, buccal views; **K-L**, CMN 32321, left M3, in **K**, occlusal and **L**, buccal views. 3-mm scale bar pertains to isolated upper incisors (**A-F)**; 4-mm scale bar pertains to isolated upper molars (**G-L).**

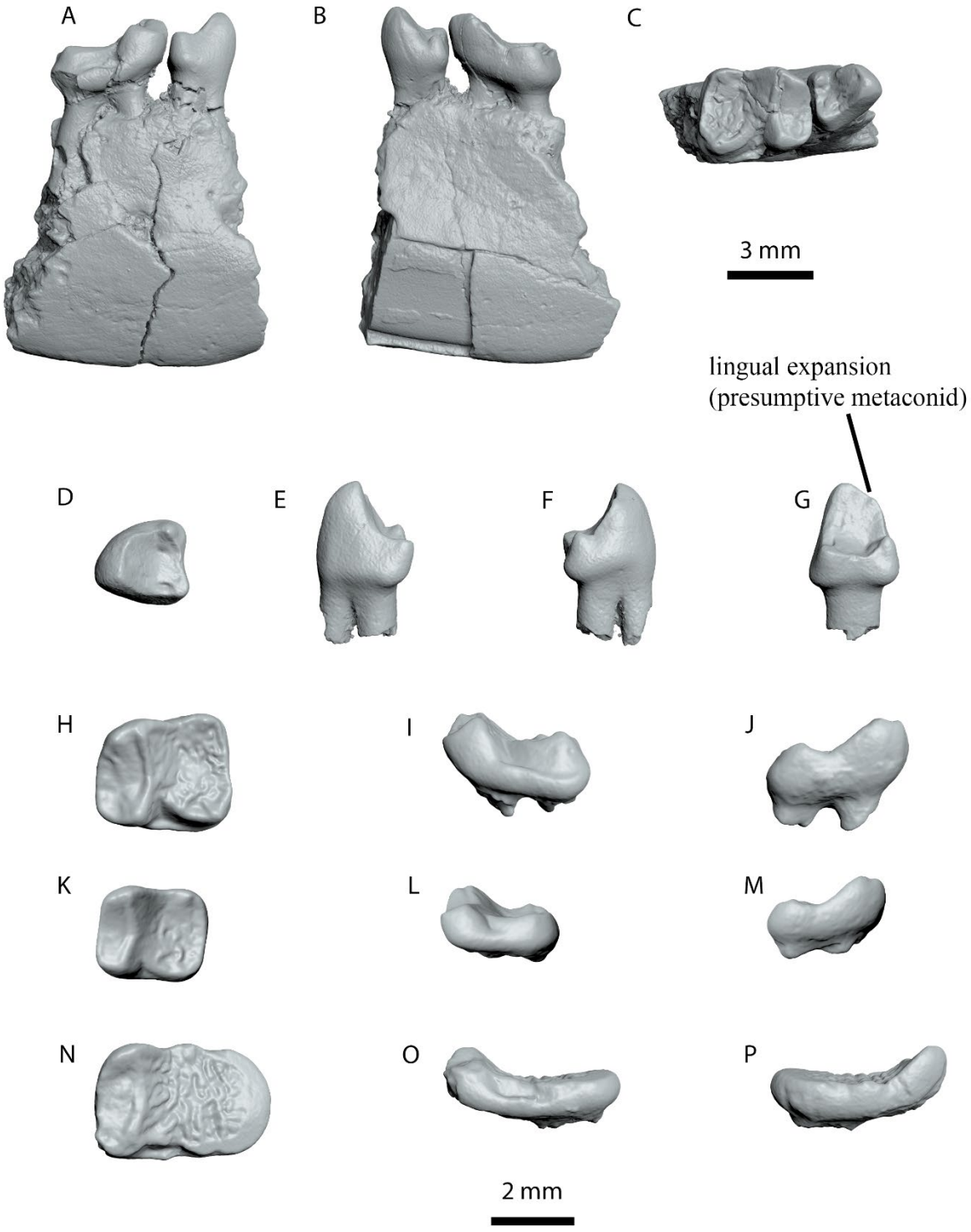

Figure 7: *Ignacius species 2* sp. nov., dentary fragment and isolated lower teeth from the Eocene Margaret Formation, Ellesmere Island, Nunavut, Canada. Images rendered from Micro CT scans. **A-C**, CMN 30837, right dentary fragment preserving p4-m1 in **A**, buccal, **B**, lingual, and **C**, occlusal views; **D-G**, CMN 30949, left p4 in **D**, occlusal, **E**, buccal, **F**, lingual, and **G**, distal views; **H-J,** CMN 30999, left m1 in **H**, occlusal, **I**, buccal, and **J**, lingual views; **K-M,** CMN 30856, right m2 (depicted as mirror image in this figure) in **K**, occlusal, **L**, buccal, and **M**, lingual views; **N-P**, CMN 30889, left m3 in **N**, occlusal, **O**, buccal, and **P**, lingual views. 3-mm scale bar pertains to dentary fragment CMN 30837 (**A-C**). 2-mm scale bar pertains to isolated lower dentition (**D-P**).

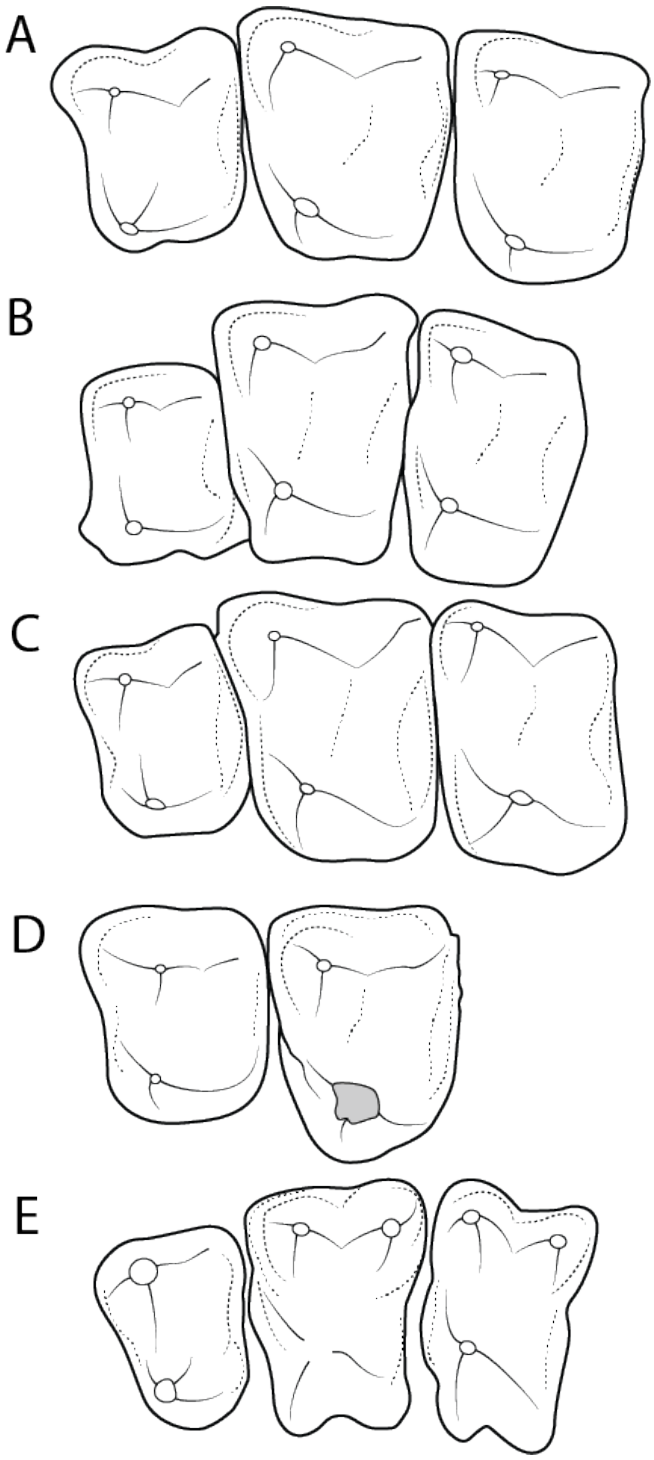

Figure 8: Upper dentition comparisons of paromomyids in occlusal view. **A**, *Ignacius frugivorus,* AMNH 17368, type, left P4-M2; **B**, *Ignacius clarkforkensis,* UM 108210, type, left P4-M2; **C**, *Ignacius graybullianus,* YPM 26004, type, right P4-M2 (reflected); **D**, *Phenacolemur archus*, UM 69237, right P4-M1 (reflected); **E**, *Paromomys farrandi* (composite), UCMP 157715 left P4, UCMP 157717, right M1 (reflected), UCMP 157715 left M2. Illustrations by Kristen Tietjen.

5. Phylogenetic Analysis

History of Phylogenetic Analyses

While phylogenetic analyses attempting to understand the higher-level relationships among plesiadapiform families have been conducted in the past (Bloch et al. 2007; Silcox 2007; Beard et al. 2016; Bloch et al. 2016), the first phylogenetic analysis focusing squarely on relationships within Paromomyidae was published by Bloch et al. (2002). This analysis was based on a restricted character-taxon matrix of only 12 dental characters and four genera (*Paromomys, Acidomomys, Ignacius,* and *Phenacolemur*) (Bloch et al. 2002). Aumont (2003), in her unpublished dissertation, provided the first in-depth phylogenetic analysis concerning paromomyids, although her analysis specifically focused on the European taxa. López-Torres and Silcox (2018) were the first to publish a detailed phylogenetic analysis with emphasis on the family Paromomyidae, and this analysis, like Aumont's (2003), focused on the clade of European paromomyids. The primary aim of López-Torres and Silcox (2018) was to understand the intrageneric relationships of the European paromomyid *Arcius*, and to place this genus within the familial context (López-Torres and Silcox 2018). While this was not a comprehensive analysis of every member of Paromomyidae, the analysis included the known species of *Arcius*, as well as the most oldest member of each paromomyid genus; *Paromomys farrandi, Edworthia leberkmoi, Acidomomys hebeticus, Phenacolemur archus,* and *Ignacius fremontensis* (López-Torres and Silcox 2018). The genus *Elwynella* was excluded from the analysis because it shows some derived characters that suggest a nested relationship within Paromomyidae and was beyond the scope of the analysis performed by López-Torres and Silcox (2018).

Phylogenetic analysis of Arctic paromomyids

Here, a phylogenetic analysis was performed to reconstruct the phylogenetic relationships of the new Arctic paromomyids with respect to other paromomyids. The unusual autapomorphies seen in the new taxa as well as their unique geographic range make their placement in the family tree of especial interest when it comes to understanding the evolutionary radiation and biogeography of the family Paromomyidae. The phylogenetic analysis aims to answer the following questions; 1) Are the Arctic taxa early diverging paromomyids that made their way into the Arctic before paromomyids diversified at mid-latitudes in North America? 2) Are the Arctic taxa highly nested within the North American paromomyid clade, indicating dispersal of taxa from mid-latitudes to the Arctic late in paromomyid evolution? 3) Are the two species found in the Arctic sister taxa or two independent paromomyid dispersals into higher latitudes? and 4) Are the Arctic taxa closely related to the European taxa, showing evidence of paromomyid migration from North America, across the North Atlantic Land Bridge, and into Europe?

Methodology

This analysis utilized 17 taxa scored for 63 dental characters. The character matrix utilized here was adapted from the matrix created by López-Torres and Silcox (2018). The full matrix is included in Appendix B. Seven taxa were added to the original matrix, including five ingroup taxa, *Ignacius species 1, Ignacius species 2, I. clarkforkensis, I. graybullianus,* and *I. frugivorus,* as well as two additional outgroup taxa, *Chronolestes simul* and *Torrejonia sirokyi*. *T. sirokyi* was selected as an additional outgroup taxon because it represents an early member of the family Palaechthonidae, a family often thought to be closely related to paromomyids (Bloch et al. 2007; Silcox 2007; Silcox et al. 2017). *Chronolestes simul* was chosen as an additional outgroup because it is thought to be a morphologically primitive plesiadapoid (Beard and Wang 1995; Beard et al. 2016). The genus *Elwynella* was again excluded from the analysis due to the

proposed nested position of this taxon within a clade other than *Ignacius*, making its phylogenetic position interesting but not particularly relevant to this study. Additionally, this genus is known from very limited fossil material and the low anatomical representation of this taxon may decrease the resolution if included in the phylogenetic analysis.

Because preliminary study suggested that the new Arctic taxa belong to the genus *Ignacius,* ten dental characters (characters 4, 14, 19, 20, 21, 22, 25, 26, 27, and 28) were added to the original matrix from López-Torres and Silcox (2018) to improve the resolution within this clade. Additional taxa and characters were scored from specimens and casts from the KUVP collection when available and scored from images in the literature when specimens/casts where unavailable. All characters were treated as unweighted and all characters except 1, 10, 16, 22, 28, and 50, were treated as unordered. A complete list of characters and coding scheme are available in Appendix A.

The phylogenetic analysis was performed using PAUP*4.0a (Swofford 2002). Two analyses were performed, one standard branch-and-bound analysis (Figure 9A) and a branch-and-bound analysis with 100 bootstrap replicates (Figure 9B). A constraint was placed on the ingroup taxa for both analyses to prevent the outgroup taxa from being placed within the ingroup. Trees were visualized using FigTree v1.4.4.

Results

The first branch-and-bound analysis with only one replicate recovered one most parsimonious tree with a tree length of 184, a consistency index (CI) of 0.44, and a retention index (RI) of 0.57 (Figure 9A). The tree recovered from this analysis was fully resolved and the relationships within the *Ignacius* clade reflect the temporal occurrence of the taxa with the earliest occurring taxon, *I. fremontensis,* diverging first, followed by *I. frugivorus, I.*

clarkforkensis, I. graybullianus, and the two Arctic taxa occupying the most nested position within the clade. Interestingly, *Acidomomys hebeticus* was recovered at the base of the *Ignacius* clade, diverging before *I. fremontensis.* Unsurprisingly, the four *Arcius* species included in this analysis form a clade, but it also includes *Phenacolemur archus* as its most basal member. The *Ignacius+Acidomomys* clade and the *Arcius+Phenacolemur* clade were recovered as sister groups to each other. *Edworthia* and *Paromomys* were recovered in a clade together as a sister group to the larger *Ignacius+Acidomomys+Arcius+Phenacolemur* clade and the earliest diverging members of the paromomyid clade.

The branch-and-bound analysis with 100 bootstrap replicates yielded a tree with a tree length of 199, a CI of 0.40, and a RI of 0.51 (Figure 9B). In the bootstrap analysis, the two Arctic taxa were recovered as sister taxa to each other in 91% of the replicates and the *Ignacius* clade was recovered as monophyletic in 57% of the replicates. The more derived species, *Ignacius sp. 1* and *2*, *I. clarkforkensis,* and *I. graybullianus* were recovered together in 64% of the replicates although the relationships between the Arctic taxa, *I. clarkforkensis* and *I. graybullianus* form a polytomy with the clade that contains the Arctic taxa. Additionally, the relationship of the two oldest species *I. frugivorus* and *I. fremontensis* was unresolved in relation to the more derived *Ignacius* taxa. Again, this analysis recovered a monophyletic *Arcius* clade with a bootstrap score of 81%. This analysis recovered a less resolved tree, and therefore a polytomy was recovered between the *Ignacius* clade, the *Arcius* clade, *Acidomomys hebeticus,* and *Phenacolemur archus;* these four groups were recovered together in 74% of the replicates. The bootstrap analysis recovered *Edworthia* and *Paromomys* as the most basal members of Paromomyidae. The outgroup taxa *Torrejonia sirokyi* and *Chronolestes simul* formed a clade in 79% of the replicates,

and *Purgatorius coracis*, one of the earliest occurring plesiadapiforms (Van Valen and Sloan 1965), was recovered as the most basal taxon in the tree.

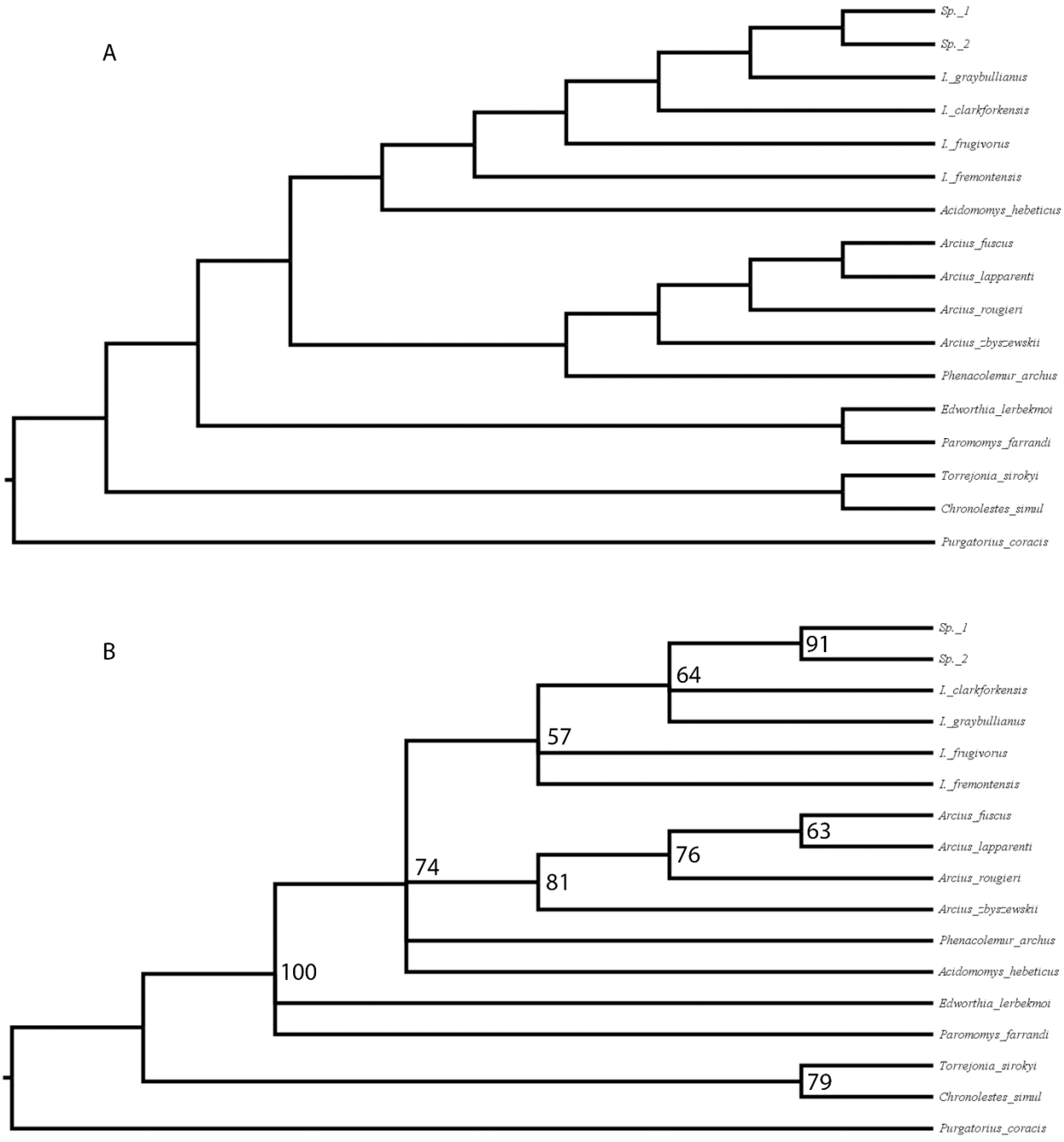

Figure 9: Results of phylogenetic analysis; A. single most parsimonious tree recovered in a branch-and-bound analysis; B. results of branch-and-bound analysis with 100 bootstrap replicates with bootstrap percentages greater than 50% shown at the respective nodes. Nodes with <50% support are collapsed.

6. Discussion and Conclusions

Phylogenetic Analysis

The results of the phylogenetic analysis corroborate the hypothesis that the two Arctic species are sister taxa that together comprise an exceptionally derived clade of *Ignacius.* This hypothesis is supported by the highly nested placement of these taxa within the *Ignacius* clade in both the single branch-and-bound analysis and the analysis with 100 bootstrap replicates. The more robust bootstrap analysis recovered the two Arctic species as sister taxa within the *Ignacius* clade in 91 replicates. This is unsurprising, as the Arctic taxa share some key synapomorphies, namely, the highly crenulated enamel and presence of a preprotocingulum on upper molars. The polytomy among *I. fremontensis, I. frugivorus* and the more derived *Ignacius* clade is also predicted as *I. fremontensis* and *I. frugivorus* are remarkably similar to one another in morphology. Of the two species, *I. fremontensis* is generally thought to be more basal, as some specimens are known to retain a p3 (Bown and Rose 1976; Bloch et al. 2002; Secord 2008). *I. fremontensis* was scored as "p3 absent" in this analysis because the specimens used for coding did not retain the plesiomorphic p3, potentially explaining the lack of resolution among these taxa in the recovered phylogeny.

The single branch-and-bound analysis placing *Acidomomys hebeticus* at the base of the *Ignacius* clade raises some interesting questions regarding the origin of this species. *Acidomomys* is contemporaneous with the derived *Ignacius* species, *I. clarkforkensis* (Bloch et al. 2002; 2007), morphologically, however, this species retains some key symplesiomorphies with the earliest occuring paromomyids, namely, the retention of a small, double rooted p3 which is only known from *Paromomys, Edworthia*, and *I. fremontensis* and the retention of a small i2 which is only present in *Paromomys* (Bloch et al. 2002; Fox et al. 2010). *Acidomomys* may, therefore,

represent the only known member of a sister group which diverged early in the evolutionary history of *Ignacius* and retained some characteristics seen only in the earliest paromomyids, well into the late Paleocene. The placement of *Acidomomys hebeticus* at the base of the *Ignacius* clade could also suggest that taxonomic revisions should be made placing this taxon within genus *Ignacius* rather than its own genus.

Interestingly, the single branch-and-bound analysis recovered *Phenacolemur archus* as the most basal member of the *Arcius* clade. This is not entirely surprising as the European paromomyids were originally described as belonging to *Phenacolemur* by Louis (1966) before the genus *Arcius* was proposed by Godinot (1984). However, the relationship between the European clade and North American paromomyids has been debated, with Russell et al. (1967) arguing for a closer relationship with *Phenacolemur* and Godinot (1984) arguing for a closer relationship with *Ignacius*. The results of the present analysis are interesting in that the recovered relationships among *Ignacius, Phenacolemur,* and *Arcius* differ from the relationships recovered in the analysis by López-Torres and Silcox (2018). The 2018 analysis (López-Torres and Silcox 2018) used TNT (Goloboff et al. 2008) to analyze their data matrix, the present analysis utilized PAUP* (Swofford 2002), which potentially explains the inconsistencies between the recovered phylogenies. Additionally, the Arctic taxa, specifically Species 1, are represented by a small number of specimens resulting in a significant number of characters that could not be scored. This could also be a contributing factor to the differences seen in the results of the two studies.

The 2018 analysis (López-Torres and Silcox 2018) recovered an *Ignacius+ Acidomomys+ Phenacolemur* clade which was the sister group to the *Arcius* clade. With the increased taxon and character sampling for the genus *Ignacius* in the present analysis, the recovered phylogeny places *Phenacolemur* as a closer relative to *Arcius* than *Ignacius.* However,

the more robust analysis performed here with 100 replicates, recovered a polytomy between the more derived paromomyid genera *Acidomomys, Arcius, Ignacius,* and *Phenacolemur*, suggesting the resolved relationships between these groups recovered in the initial branch-and-bound anlysis were weakly supported. Thus, a more comprehensive analysis including additional species of *Phenacolemur* as well as additional characters would be necessary to disentangle the contentious relationship of these taxa.

Unsurprisingly, in both analyses conducted here, *Paromomys farrandi* and *Edworthia lerbekmoi* were recovered as the earliest diverging paromomyids, as in the prior analysis by López-Torres and Silcox (2018) This is consistent with the temporal distributions and plesiomorphic morphology seen in these two taxa.

Biogeography

The results of the phylogenetic analysis raise some interesting implications for the evolution of the genus *Ignacius.* The highly nested position of the Arctic taxa within a clade previously known only from mid-latitudes of North America suggest the new species from Ellesmere Island dispersed there from North American mid-latitudes. The highly nested position of the two new taxa rule out the hypothesis that these were early diverging paromomyids that dispersed into the Arctic region before the diversification of paromomyids at mid-latitudes. The hypothesis of a northward dispersal from mid-latitudes is further supported by the occurrence dates of members of the *Ignacius* clade, as the morphologically primitive species are known primarily from the Torrejonian and Tiffanian, whereas the more derived taxa, *I. clarkforkensis* and *I. graybullianus* (from the middle Clarkforkian and early Wasatchian respectively) (Bown and Rose 1976; Scott 2003), show a closer relationship with the Arctic taxa which occur in late Wasatchian strata on Ellesmere Island (Eberle and Greenwood 2012). The temporal and

phylogenetic position of the two new species suggest they are sister taxa to the early Wasatchian *I. graybullianus*.

The northward dispersal of *Ignacius* may have been in response to global climatic changes at the time. The Early Eocene Climatic Optimum (EECO) was a global climatic event that took place from ca. 53–50 Ma, lasted approximately 3 Ma, and was marked by a mean annual temperature of ~23ºC at mid-latitudes in North America (Wilf 2000; Woodburne et al. 2009). Global warming events during the early Paleogene have been linked with mammalian faunal turnover and migration in North America (Chew 2009; Woodburne et al. 2009), and Beard (1998; 2002) suggested periods of global warming have facilitated the dispersal of mammalian taxa into higher latitudes as latitudinal temperature gradients recede in response to increased temperatures. The evidence of mammalian dispersal in response to global warming events along with the temporal correlation between the Arctic *Ignacius* species and the EECO, support a hypothesis in which rising temperatures in the early Eocene facilitated a northward dispersal of *Ignacius* to Ellesmere Island, where they subsequently diversified into at least two separate species. Additionally, the two species from Ellesmere Island are the youngest occurring members of the genus *Ignacius* (omitting the single tooth from the Chadronian with contentious affinities). This suggests that perhaps paromomyids preferred the cooler climate present at higher latitudes during the EECO rather than the warm, tropical conditions at mid-latitudes. This is further corroborated by the absence of paromomyids in the Red Hot local fauna of Mississippi which dates to the early Wasatchian and would have represented a much warmer environment (Beard and Dawson 2009). This may indicate the *Ignacius* species populating Ellesmere Island during the late Wasatchian were relictual while the species in lower latitudes of North America went extinct as the environment warmed during the early Eocene.

The phylogenetic position of the Arctic *Ignacius* species suggest they are not closely related to the European clade, *Arcius*, even though it has been hypothesized that the ancestors of *Arcius* dispersed from North America to Europe via the North Atlantic land bridge which was partially comprised by what is now Ellesmere Island and Greenland (Eberle and Greenwood 2012; López-Torres and Silcox 2018). The relatively distant phylogenetic relationship between the Arctic paromomyids and *Arcius* suggest there may have been a separate dispersal event of North American paromomyids (perhaps a relative of *Phenacolemur* given the placement of this genus in the present analysis*)* into the Arctic region and then eastward across the North Atlantic land bridge into Europe, giving rise to the genus *Arcius*, although no fossils of *Phenacolemur* are presently known from the Arctic.

Further insight into the biogeography of paromomyids and especially *Ignacius* could be gleaned if the undescribed specimens recovered from Shandong Province, China (Tong and Wang 1998) were included in the analysis. Very little is known about this taxon, as it has been mentioned but never formally described in the literature; it has, however, been referred to as a new species of *Ignacius* (Tong and Wang 1998). This raises a plethora of additional questions regarding the biogeography and overall evolutionary radiation of paromomyids and where the Asian taxon fits phylogenetically and temporally in relation to the rest of the family. Does this taxon represent a more basal *Ignacius* species or is it nested within the clade as seen in the Arctic taxa?

Future Research

The interesting autapomorphies seen in the dentition of the paromomyid species from Ellesmere Island, along with the unique ecosystem present in this area during the Eocene, raises questions regarding how these mammals (whose modern relatives live in latitudes surrounding

the equator) survived through the approximately six months of darkness of Arctic winters. As the EECO represents the highest temperatures of the most prolonged global warming event during the Cenozoic (Woodburne et al. 2009), Arctic winters would have reached minimum temperatures at or just above freezing (Eberle et al. 2010; West et al. 2015, 2020). The highly crenulated enamel seen on the teeth of the Ellesmere Island paromomyids is similar to the crenulation seen in some modern day primates that are predominately hard object feeders, like pitheciid platyrrhines (Winchester et al. 2014). This may suggest the Arctic paromomyids may have been subsisting off tough shelled fruits or perhaps tough leaf litter as seen in the pantodont *Coryphodon* from the Canadian Arctic (Eberle et al. 2020). This seems to correspond with the conclusion of a previous dental topography analysis of paromomyids conducted by López-Torres et al. (2018) where the authors found that dental topography of *Ignacius* was consistent with the topography of known frugivores. An enlightening future study could include the Arctic taxa, additional species of *Ignacius*, as well as known frugivorous and hard object-feeding primates in a similar dental topography analysis to elucidate the dietary adaptations of the new species. Analysis of the paleobotanical literature of Ellesmere Island could potentially reveal candidates for paromomyid dietary resources. This also raises a question about seasonality of fruits/nuts in an environment where very little to no photosynthesis occurs during the winter months, causing potential food shortages for the paromomyids residing there. Is the evolution of highly crenulated enamel in Arctic paromomyids driven by the need to resort to fallback foods during seasons of scarce or no fruit production?

Additionally, the Arctic paromomyids express a unique pattern of dental wear on their upper incisors. Whereas other paromomyids generally express apical wear on the upper incisor cusps, the cusps of the Arctic paromomyid upper incisors are unworn, while the lingual surface

of the incisors are highly worn. Some authors (Beard 1990; 1991; Boyer and Bloch 2008) suggest paromomyids may have been adapted to feeding on exudates using their procumbent, lower incisors to access tree sap. Future analyses of upper and lower incisor wear patterns on exudate-feeding mammals like callitrichine primates (Garber 1992) and the marsupial sugar glider, *Petaurus* (Smith 1982), could potentially provide evidence for exudate-feeding in the Arctic paromomyids. Previous studies have shown that exudate-feeding by extant callitrichine primates is highly seasonal, with most exudate-feeding occurring during the dry months when fruits are scarce (Garber 1992). Again, analysis of the paleobotanical literature of Ellesmere Island could help elucidate whether tree sap was available to paromomyids and whether the availability of sap was seasonal. Paromomyids may have been feeding on abundant fruits during the warm months and falling back on exudates when fruit was scarce, or relying on soft fruits and exudates as a primary food source during the summer months, while falling back on tough plant materials during the winter months, as has been shown to occur in Eocene Arctic *Coryphodon* (Eberle et al. 2009). The unique dental morphology of the Arctic paromomyids that may have allowed them to access fall-back foods and their hypothesized ability to feed on exudates may explain why no other members of the clade Primatomorpha have been recovered from Ellesmere Island. The adaptations of these paromomyids may have allowed them to access unique food sources that were inaccessible to other Primatomorphs.

Conclusions

The Eocene strata of the Margaret Formation on Ellesmere Island sample a unique, temperate ecosystem unlike any seen today with its warm, greenhouse temperatures and polar light regime (Eberle and Greenwood 2012; Eberle and Eberth 2015). This unique environment has produced equally unique extinct mammalian taxa like the paromomyid plesiadapiform

Ignacius (West and Dawson 1978; Dawson 1990; Eberle and Greenwood 2012). The phylogenetic position of the two new species of *Ignacius* recovered in this study suggests these species are closely related to *Ignacius graybullianus* and *Ignacius clarkforkensis* from the latest Paleocene and earliest Eocene of Wyoming. The results of this analysis along with temporal occurrence data, suggest that a derived species of *Ignacius* dispersed into northern latitudes during the EECO, where they colonized Ellesmere Island and diversified into two distinct species with unique adaptations for surviving in a warm temperate ecosystem with a polar light regime. Additionally, the analysis suggests there may have been a separate dispersal event of paromomyids through the Arctic region around this time period, as the European paromomyid *Arcius* was not recovered as a close relative of the paromomyids found on Ellesmere Island, but has been hypothesized as dispersing to Europe from North America through the North Atlantic land bridge (López-Torres and Silcox 2018).

Future research will focus on elucidating the diet of the new *Ignacius* taxa based on dental topography analyses as well as the paleobotanical record of Ellesmere Island. Additional analyses like enamel microwear (Ungar et al. 2006), enamel microstructure (Eberle et al. 2020), and carbon isotope anlysis (Cerling et al. 2003) could also help elucidate the diet of these unique species. These new taxa offer a unique perspective on primatomorph adaptation in the face of increasing global temperatures during the EECO. As no other living or extinct primatomorphs have been found at such high latitudes, this research could help shed light on how modern day primatomorphs could respond to the ongoing global warming event observed today.

References

Alroy, John. 1999. “The Fossil Record of North American Mammals: Evidence for a Paleocene Evolutionary Radiation.” Edited by P. Waddell. *Systematic Biology* 48 (1): 107–18. https://doi.org/10.1080/106351599260472.

Aumont, Adeline. 2003. “Systématique et Phylogénie Des Paromomyidés Européens:(Eocène-Plésiadapiformes, Mammifères).” PhD Thesis, Paris, Muséum national d’histoire naturelle.

Beard, K. Christopher. 1990. “Gliding Behaviour and Palaeoecology of the Alleged Primate Family Paromomyidae (Mammalia, Dermoptera).” *Nature* 345 (6273): 340–41.

———. 1991. “Vertical Postures and Climbing in the Morphotype of Primatomorpha: Implications for Locomotor Evolution in Primate History.” *Origines de La Bipédie Chez Les Hominidés*, 79–87.

———. 1993. “Phylogenetic Systematics of the Primatomorpha, with Special Reference to Dermoptera.” In *Mammal Phylogeny*, edited by Frederick S. Szalay, Michael J. Novacek, and Malcolm C. McKenna, 129–50. New York, NY: Springer New York. https://doi.org/10.1007/978-1-4613-9246-0_10.

———. 1998. “East of Eden: Asia as an Important Center of Taxonomic Origination in Mammalian Evolution.” *Bulletin of the Carnegie Museum of Natural History* 34: 5–39.

———. 2002. “East of Eden at the Paleocene/Eocene Boundary.” *Science* 295 (5562): 2028–29.

Beard, K. Christopher, and Mary R. Dawson. 2009. “Early Wasatchian Mammals of the Red Hot Local Fauna, Uppermost Tuscahoma Formation, Lauderdale County, Mississippi.” *Annals of Carnegie Museum* 78 (3): 193–243. https://doi.org/10.2992/007.078.0301.

Beard, K. Christopher, and Jingwen Wang. 1995. “The First Asian Plesiadapoids (Mammalia: Primatomorpha).” *Annals of Carnegie Museum* 64: 1–33.

Beard, K Christopher, NI Xi-Jun, WANG Yuan-Qing, MENG Jin, and Daniel L Gebo. 2016. “Dentition of Subengius Mengi (Mammalia: Plesiadapoidea) and a Reassessment of the Phylogenetic Relationships of Asian Carpolestidae.” *Vertebrata PalAsiatica* 54 (2): 31.

Bloch, Jonathan I., Doug M. Boyer, Philip D. Gingerich, and Gregg F. Gunnell. 2002. “New Primitive Paromomyid from the Clarkforkian of Wyoming and Dental Eruption in Plesiadapiformes.” *Journal of Vertebrate Paleontology* 22 (2): 366–79. https://doi.org/10.1671/0272-4634(2002)022[0366:NPPFTC]2.0.CO;2.

Bloch, Jonathan I., Stephen G.B. Chester, and Mary T. Silcox. 2016. “Cranial Anatomy of Paleogene Micromomyidae and Implications for Early Primate Evolution.” *Journal of Human Evolution* 96 (July): 58–81. https://doi.org/10.1016/j.jhevol.2016.04.001.

Bloch, Jonathan I, and Philip D. Gingerich. 1998. “Carpolestes Simpsoni, New Species (Mammalia, Proprimates) From the Late Paleocene of the Clarks Fork Basin, Wyoming,” 34.

Bloch, Jonathan I., Mary T. Silcox, Doug M. Boyer, and Eric J. Sargis. 2007. “New Paleocene Skeletons and the Relationship of Plesiadapiforms to Crown-Clade Primates.” *Proceedings of the National Academy of Sciences* 104 (4): 1159–64.

Bown, Thomas M., and Kenneth D. Rose. 1976. “New Early Tertiary Primates and a Reappraisal of Some Plesiadapiformes.” *Folia Primatologica* 26 (2): 109–38. https://doi.org/10.1159/000155734.

Boyer, Doug M., and Jonathan I. Bloch. 2008. “Evaluating the Mitten-Gliding Hypothesis for Paromomyidae and Micromomyidae (Mammalia,‘Plesiadapiformes’) Using Comparative

Functional Morphology of New Paleogene Skeletons." In *Mammalian Evolutionary Morphology*, 233–84. Springer.

Cerling, Thure E., John M. Harris, and Benjamin H. Passey. 2003. "Diets of East African Bovidae Based on Stable Isotope Analysis." *Journal of Mammalogy* 84 (2): 456–70.

Chew, Amy E. 2009. "Paleoecology of the Early Eocene Willwood Mammal Fauna from the Central Bighorn Basin, Wyoming." *Paleobiology* 35 (1): 13–31.

Clemens, William A, and Gregory P Wilson. 2009. "Early Torrejonian Mammalian Local Faunas from Northeastern Montana, U.S.A.," 48.

Dawson, Mary. 1990. "Terrestrial Vertebrates from the Tertiary of Canada's Arctic Islands." In *Canada's Missing Dimension : Science and History in the Canadian Arctic Islands*, edited by C.R. Harington. Vol. 1. Ottawa : Canadian Museum of Nature,. https://doi.org/10.5962/bhl.title.52115.

Eberle, J., H. Fricke, and J. Humphrey. 2009. "Lower-Latitude Mammals as Year-Round Residents in Eocene Arctic Forests." *Geology* 37 (6): 499–502. https://doi.org/10.1130/G25633A.1.

Eberle, J. J., and D. R. Greenwood. 2012. "Life at the Top of the Greenhouse Eocene World--A Review of the Eocene Flora and Vertebrate Fauna from Canada's High Arctic." *Geological Society of America Bulletin* 124 (1–2): 3–23. https://doi.org/10.1130/B30571.1.

Eberle, Jaelyn J. 2005. "A New 'Tapir' from Ellesmere Island, Arctic Canada — Implications for Northern High Latitude Palaeobiogeography and Tapir Palaeobiology." *Palaeogeography, Palaeoclimatology, Palaeoecology* 227 (4): 311–22. https://doi.org/10.1016/j.palaeo.2005.06.008.

Eberle, Jaelyn J., and David A. Eberth. 2015. "Additions to the Eocene Perissodactyla of the Margaret Formation, Eureka Sound Group, Ellesmere Island, Arctic Canada." *Canadian Journal of Earth Sciences* 52 (2): 123–33.

Eberle, Jaelyn J., Henry C. Fricke, John D. Humphrey, Logan Hackett, Michael G. Newbrey, and J. Howard Hutchison. 2010. "Seasonal Variability in Arctic Temperatures during Early Eocene Time." *Earth and Planetary Science Letters* 296 (3–4): 481–86. https://doi.org/10.1016/j.epsl.2010.06.005.

Eberle, Jaelyn J., Wighart von Koenigswald, and David A. Eberth. 2020. "Using Tooth Enamel Microstructure to Identify Mammalian Fossils at an Eocene Arctic Forest." Edited by Adam Csank. *PLOS ONE* 15 (9): e0239073. https://doi.org/10.1371/journal.pone.0239073.

Eberle, Jaelyn, and Malcolm Mckenna. 2007. "The Indefatigable Mary R. Dawson: Arctic Pioneer," 12.

Foreman, Brady Z., Paul L. Heller, and Mark T. Clementz. 2012. "Fluvial Response to Abrupt Global Warming at the Palaeocene/Eocene Boundary." *Nature* 491 (7422): 92–95. https://doi.org/10.1038/nature11513.

Fox, Richard C, Craig S Scott, and Brian D Rankin. 2010. "Edworthia Lerbekmoi, a New Primitive Paromomyid Primate from the Torrejonian (Early Paleocene) of Alberta, Canada," 12.

Francis, Jane E. 1988. "A 50-Million-Year-Old Fossil Forest from Strathcona Fiord, Ellesmere Island, Arctic Canada: Evidence for a Warm Polar Climate." *Arctic* 41 (4): 314–18. https://doi.org/10.14430/arctic1738.

Garber, Paul A. 1992. “Vertical Clinging, Small Body Size, and the Evolution of Feeding Adaptations in the Callitrichinae.” *American Journal of Physical Anthropology* 88 (4): 469–82.

Gazin, C. L. 1971. “Paleocene Primates from the Shotgun Member of the Fort Union Formation in the Wind River Basin, Wyoming.” *Proceedings of the Biological Society of Washington* 84 (3): 13–38.

Godinot, Marc. 1984. “Un Nouveau Genre de Paromomyidae (Primates) de l’Eocène Inférieur d’Europe.” *Folia Primatologica* 43 (2–3): 84–96.

Goloboff, Pablo A., James S. Farris, and Kevin C. Nixon. 2008. “TNT, a Free Program for Phylogenetic Analysis.” *Cladistics* 24 (5): 774–86.

Gunnell, Gregg Frederick. 1986. “Evolutionary History of Microsyopoidea (Mammalia, Primates?) And the Relationship of Plesiadapiformes to Primates.” PhD Thesis, University of Michigan.

Kay, Richard F., J. G. M. Thewissen, and Anne D. Yoder. 1992. “Cranial Anatomy of Ignacius Graybullianus and the Affinities of the Plesiadapiformes.” *American Journal of Physical Anthropology* 89 (4): 477–98.

Kay, Richard F., Richard W. Thorington, and Peter Houde. 1990. “Eocene Plesiadapiform Shows Affinities with Flying Lemurs Not Primates.” *Nature* 345 (6273): 342–44.

Kihm, Allen, and Matthew Tornow. 2014. “First Occurrence of Plesiadapiform Primates from the Chadronian (Latest Eocene)” 9 (4): 7.

Kraus, Mary J., Francesca A. McInerney, Scott L. Wing, Ross Secord, Allison A. Baczynski, and Jonathan I. Bloch. 2013. “Paleohydrologic Response to Continental Warming during the Paleocene–Eocene Thermal Maximum, Bighorn Basin, Wyoming.” *Palaeogeography, Palaeoclimatology, Palaeoecology* 370 (January): 196–208. https://doi.org/10.1016/j.palaeo.2012.12.008.

Krishtalka, L. 1978. “Paleontology and Geology of the Badwater Creek Area, Central Wyoming Part 15. Review of the Late Eocene Primates from Wyoming and Utah, and the Plesitarsiiformes,” 28.

Lillegraven, Jason A., and Jaelyn J. Eberle. 1999. “Vertebrate Faunal Changes through Lancian and Puercan Time in Southern Wyoming.” *Journal of Paleontology* 73 (4): 691–710. https://doi.org/10.1017/S0022336000032510.

López-Torres, Sergi, Keegan R. Selig, Kristen A. Prufrock, Derrick Lin, and Mary T. Silcox. 2018. “Dental Topographic Analysis of Paromomyid (Plesiadapiformes, Primates) Cheek Teeth: More than 15 Million Years of Changing Surfaces and Shifting Ecologies.” *Historical Biology* 30 (1–2): 76–88.

López-Torres, Sergi, and Mary T. Silcox. 2018. “The European Paromomyidae (Primates, Mammalia): Taxonomy, Phylogeny, and Biogeographic Implications.” *Journal of Paleontology* 92 (5): 920–37. https://doi.org/10.1017/jpa.2018.10.

López-Torres, Sergi, Mary T. Silcox, and Patricia A. Holroyd. 2018. “New Omomyoids (Euprimates, Mammalia) from the Late Uintan of Southern California, USA, and the Question of the Extinction of the Paromomyidae (Plesiadapiformes, Primates).” *Palaeontologia Electronica* 21 (3). https://doi.org/10.26879/756.

Louis, P. 1966. “Note Sur Un Nouveau Gisement Situé à Condé En Brie (Aisne) et Renfermant Des Restes de Mammifères de l’Éocène Inférieur.” *Ann. Sci. Univ. Reims et ARERS* 4: 108–18.

Matthew, W D, and Walter Granger. 1915. “Article XIV.- A Revision of the Lower Eocene Wasatch and Wind River Faunas.” 58.

Matthew, William Diller, and Walter Granger. 1921. “New Genera of Paleocene Mammals." American Museum Novitates; No. 13.

Miall, Andrew D. 1986. “The Eureka Sound Group (Upper Cretaceous-Oligocene), Canadian Arctic Islands.” *Bulletin of Canadian Petroleum Geology* 34 (2): 240–70.

Prufrock, Kristen A., Doug M. Boyer, and Mary T. Silcox. 2016. “The First Major Primate Extinction: An Evaluation of Paleoecological Dynamics of North American Stem Primates Using a Homology Free Measure of Tooth Shape.” *American Journal of Physical Anthropology* 159 (4): 683–97.

Reinhardt, Lutz, Werner von Gosen, Karsten Piepjohn, Andreas Lückge, and Mark Schmitz. 2017. “The Eocene Thermal Maximum 2 (ETM-2) in a Terrestrial Section of the High Arctic: Identification by U-Pb Zircon Ages of Volcanic Ashes and Carbon Isotope Records of Coal and Amber (Stenkul Fiord, Ellesmere Island, Canada).” In *EGU General Assembly Conference Abstracts*, 8145.

Ricketts, B. D. 1986. “New Formations in the Eureka Sound Group. Canadian Arctic Islands.” *Geological Survey of Canada*, 363–74.

Robinson, Peter. 1968. “The Paleontology and Geology of the Badwater Creek Area, Central Wyoming.,” 41.

Rose, Kenneth D., and Thomas M. Bown. 1982. “New Plesiadapiform Primates from the Eocene of Wyoming and Montana.” *Journal of Vertebrate Paleontology* 2 (1): 63–69. https://doi.org/10.1080/02724634.1982.10011918.

Rose, Kenneth David. 1981. “The Clarkforkian Land-Mammal Age and Mammalian Faunal Composition across the Paleocene-Eocene Boundary.”

———. 2006. *The Beginning of the Age of Mammals*. Baltimore: Johns Hopkins Univ. Press.

Russell, Donald E., P Louis, and D Savage. 1967. “Primates of the French Early Eocene.” *University of California Publications in the Geological Sciences* 73: 1–46.

Schiebout, Judith Ann. 1974. “Vertebrate Paleontology and Paleoecology of Paleocene Black Peaks Formation, Big Bend National Park, Texas.” 104.

Scott, Craig S. 2003. “Late Torrejonian (Middle Paleocene) Mammals from South Central Alberta, Canada.” *Journal of Paleontology* 77 (4): 24.

Scott, Craig S., Daniel N. Spivak, and Arthur R. Sweet. 2013. “First Mammals from the Paleocene Porcupine Hills Formation of Southwestern Alberta, Canada.” Edited by Hans Sues. *Canadian Journal of Earth Sciences* 50 (3): 355–78. https://doi.org/10.1139/e2012-044.

Secord, Ross. 2008. “The Tiffanian Land-Mammal Age (Middle and Late Paleocene) in the Northern Bighorn Basin, Wyoming,” 209.

Silcox, M. T. 2007. “Primate Taxonomy, Plesiadapiforms, and Approaches to Primate Origins.” In *PRIMATE ORIGINS: Adaptations and Evolution*, edited by Matthew J. Ravosa and Marian Dagosto, 143–78. Boston, MA: Springer US. https://doi.org/10.1007/978-0-387-33507-0_5.

Silcox, Mary T., Jonathan I. Bloch, Doug M. Boyer, Stephen GB Chester, and Sergi López-Torres. 2017. “The Evolutionary Radiation of Plesiadapiforms.” *Evolutionary Anthropology: Issues, News, and Reviews* 26 (2): 74–94.

Simpson, George Gaylord. 1935. “The Tiffany Fauna, Upper Paleocene.” *American Museum Novitates*, no. 817: 28.

———. 1940. “Studies on the Earliest Primates. Bulletin of the AMNH; v. 77, Article 4.”
———. 1955. “The Phenacolemuridae, New Family of Early Primates. Bulletin of the AMNH; v. 105, Article 5.”
Smith, A. P. 1982. “Diet and Feeding Strategies of the Marsupial Sugar Glider in Temperate Australia.” *The Journal of Animal Ecology*, 149–66.
Swofford, David L. 2002. “Laboratory of Molecular Systematics Smithsonian Institution,” 143.
Tong, Yongsheng, and J Wang. 1998. “A Preliminary Report on the Early Eocene Mammals of the Wutu Fauna, Shandong Province, China.” *Bulletin of Carnegie Museum of Natural History* 34: 186–93.
Tozer, E. T. 1963. “Mesozoic and Tertiary Stratigraphy.” In *Geology of the North-Central Part of the Arctic Archipelago, NWT (Operation Franklin). Edited by YO Fortier et al. Geological Survey of Canada, Memoir*, edited by Y. O. Fortier, 320:74–95.
Troelsen, J. C. 1950. “Contributions to the Geology of Northwest Greenland, Ellesmere.” *Island, and Axel Heiberg Island: Meddelelser Om Grønland* 149 (7).
Ungar, Peter S., Christopher A. Brown, Torbjorn S. Bergstrom, and Alan Walker. 2006. “Quantification of Dental Microwear by Tandem Scanning Confocal Microscopy and Scale-Sensitive Fractal Analyses.” *Scanning* 25 (4): 185–93. https://doi.org/10.1002/sca.4950250405.
Van Valen, Leigh, and Robert Sloan. 1965. “The Earliest Primates,” 4.
Von Gosen, W., L. Reinhardt, K. Piepjohn, and M. D. Schmitz. 2019. “Paleogene Sedimentation and Eurekan Deformation in the Stenkul Fiord Area of Southeastern Ellesmere Island (Canadian Arctic): Evidence for a Polyphase History.” *Circum-Arctic Structural Events: Tectonic Evolution of the Arctic Margins and Trans-Arctic Links with Adjacent Orogens* 541: 325.
West, Christopher K., David R. Greenwood, and James F. Basinger. 2015. “Was the Arctic Eocene ‘Rainforest’ Monsoonal? Estimates of Seasonal Precipitation from Early Eocene Megafloras from Ellesmere Island, Nunavut.” *Earth and Planetary Science Letters* 427 (October): 18–30. https://doi.org/10.1016/j.epsl.2015.06.036.
West, Christopher K., David R. Greenwood, Tammo Reichgelt, Alexander J. Lowe, Janelle M. Vachon, and James F. Basinger. 2020. “Paleobotanical Proxies for Early Eocene Climates and Ecosystems in Northern North America from Middle to High Latitudes.” *Climate of the Past* 16 (4): 1387–1410. https://doi.org/10.5194/cp-16-1387-2020.
West, R M, and M R Dawson. 1978. “Vertebrale Paleontology and the Cenozoic History of the North Atlantic Region,” 17.
West, R. M., M. R. Dawson, L. J. Hickey, and A. D. Miall. 1981. “Upper Cretaceous and Paleogene Sedimentary Rocks, Eastern Canadian Arctic and Related North Atlantic Areas.”
Wilf, Peter. 2000. “Late Paleocene–Early Eocene Climate Changes in Southwestern Wyoming: Paleobotanical Analysis.” *Geological Society of America Bulletin* 112 (2): 292–307.
Wilson Mantilla, Gregory P., Stephen G. B. Chester, William A. Clemens, Jason R. Moore, Courtney J. Sprain, Brody T. Hovatter, William S. Mitchell, Wade W. Mans, Roland Mundil, and Paul R. Renne. 2021. “Earliest Palaeocene Purgatoriids and the Initial Radiation of Stem Primates.” *Royal Society Open Science* 8 (2): 210050. https://doi.org/10.1098/rsos.210050.
Winchester, Julia M., Doug M. Boyer, Elizabeth M. St. Clair, Ashley D. Gosselin-Ildari, Siobhán B. Cooke, and Justin A. Ledogar. 2014. “Dental Topography of Platyrrhines and

Prosimians: Convergence and Contrasts." *American Journal of Physical Anthropology* 153 (1): 29–44.

Woodburne, M. O., G. F. Gunnell, and R. K. Stucky. 2009. "Climate Directly Influences Eocene Mammal Faunal Dynamics in North America." *Proceedings of the National Academy of Sciences* 106 (32): 13399–403. https://doi.org/10.1073/pnas.0906802106.

Appendix A: List of Characters and Coding Scheme Used in Phylogenetic Analysis

Characters in blue are additions to the original matrix by López-Torres and Silcox (2018)

General Characters

1. Enamel crenulation in upper/lower molar basins (ordered)
   0: Absent
   1: Moderate crenulation in some/all molars
   2: Strong crenulation in all molar basins

Upper incisors

2. Presence of posterocone on I1
   0: Absent
   1: Present
3. Relative height anterocone/mediocone on I1
   0: Anterocone taller than mediocone
   1: Mediocone taller than anterocone
4. Position of the laterocone in relation to the anterocone
   0: Laterocone positioned at the base of anterocone
   1: Laterocone approaching the height of the anterocone

Upper premolars

5. Presence of P2
   0: Absent
   1: Present
6. Presence of metacone on P4
   0: Absent
   1: Present
7. Presence of a molariform P4
   0: P4 with a metacone significantly smaller than the paracone and no expanded distolingual basin
   1: P4 with a metacone approaching in size to the paracone and an expanded distolingual basin
8. Presence of precingulum on P4
   0: Absent
   1: Present
9. Presence of parastyle on P4
   0: Absent
   1: Present
10. Shape of P4 (ordered)
    0: T-shaped
    1: Triangular
    2: Quadrangular
11. Mesial parastylar expansion on P4
    0: Projecting beyond the mesial border
    1: Not projecting
12. Acuteness of P4 cusps
    0: Acute

1: Bulbous

13. Height of postprotocingulum on P4
    0: Low (crest dips closer to the roots)
    1: High (crest stays near the tip of the protocone in height)

Upper molars

14. Position of zygomatic arch in relation to M1
    0: Root of zygomatic begins distal to the mesial border of M1
    1: Root of zygomatic begins at mesial edge of M1
15. Depth of distolingual basin on M1-2
    0: Shallow
    1: Deep
16. Presence of conules on M1-2 (ordered)
    0: Both conules present
    1: Metaconules absent
    2: Both conules absent
17. Parastylar expansion on M1-2
    0: No expansion
    1: Expanded
18. Outline of M1
    0: Squared
    1: Rectangular and narrow
19. Shape of the ectoflexus (buccal margin) on M1-2
    0: invaginated ectoflexus
    1: non-invaginated ectoflexus
20. Slope of post-protocingulum
    0: steep slope
    1: gradual slope
21. Presence of a pre-protocingulum
    0: absent
    1: present
22. Morphology of the precingulum and mesiobuccal cingulum on M^{1-2} (ordered)
    0: No precingulum
    1: Short precingulum (precingulum runs buccally from the base of the protocone but ends at or before paraconule), no overlap with the mesiobuccal cingulum
    2: long precingulum (precingulum runs buccally from the base of the protocone past the paraconule), no overlap with the mesiobuccal cingulum
    3: long precingulum that overlaps the mesiobuccal cingulum creating a “stair step” morphology
23. Depth of trigon basin on M1-2
    0: Shallow
    1: Deep
24. Presence of postmetaconule crista on M1-2
    0: Absent
    1: Present
25. V shaped postparacone/prematacone cristae on M1
    0: Absent

1: Present
26. Height of metacone in relation to height of the paracone of M1
0: Paracone and metacone equal in heigh
1: Metacone significantly shorter than paracone
27. Expansion of mesiolabial corner on M3
0: Not expanded, buccal border is straight
1: Expanded
28. Expansion of distolingual basin on M3 (ordered)
0: No expansion (distolingual basin does not expand beyond metacone)
1: Slightly expanded (distolingual basin expands slightly beyond metacone)
2: Significantly expanded (distolingual basin becomes a hypocone lobe)

Lower canine

29. Presence of C1
0: Present
1: Absent

Lower premolars

30. Presence of P2
0: Present
1: Absent
31. Presence of P3
0: Present
1: Absent
32. Trigonid/talonid width proportion on P4
0: Talonid as wide as or wider than trigonid
1: Talonid narrower than trigonid
33. P4/M1 width proportion
0: P4 narrower than M1
1: P4 of approximately the same width as M1
34. Width at the base of the P4 protoconid
0: Narrowly based protoconid
1: Broadly based protoconid
35. Presence of a mesial bulge in the base of the P4 protoconid
0: Absent
1: Present
36. P4/M1 area proportion
0: Small P4 area compared to M1 area
1: Similar
37. Relative mesiodistal length of P4 to M1
0: P4 shorter than M1
1: P4 equal or longer than M1
38. Morphology of the hypoflexid
0: Distinct, deep
1: Not distinct, shallow
39. Presence of paracristid
0: Present
1: Absent

40. Relative length of the talonid compared to the length of the tooth
    0: Relatively short talonid (less than 26% of the tooth length)
    1: Relatively long talonid (more than 26% of the tooth length)
41. Presence of a crest connecting the protoconid and the hypoflexid fold (prehypoflexid cristid)
    0: Absent
    1: Present
42. Presence of a metaconid
    0: Absent
    1: Lingual expansion of the protoconid (not yet a full metaconid)
    2: Present

Lower molars

43. Length of trigonid
    0: Trigonids become less mesiodistally compressed from M1 to M3, or there is no change
    1: Trigonids become more mesiodistally compressed from M1 to M3
44. Shape of the protocristid on M1
    0: V-shaped
    1: Slightly concave
45. Presence of distal cingulid on M1 and M2
    0: Absent
    1: Present
46. Presence of hypoconulid on M1 and M2
    0: Absent
    1: Present
47. Presence of buccal cingulid on M1 and M2 trigonids
    0: Absent
    1: Present
48. Presence of buccal cingulid on M1 and M2 talonids
    0: Absent
    1: Present
49. Shape of the M1 trigonid basin
    0: Semicircular
    1: Squared
    2: Triangular
50. Mesial inflection of the M1 and M2 trigonids (ordered)
    0: Absent/weak
    1: Somewhat pronounced
    2: Very pronounced
51. Relative height of the hypoconid compared to the entoconid on M1
    0: Hypoconid taller than entoconid
    1: Subequal
    2: Entoconid taller than hypoconid
52. Relative height of the protoconid compared to the metaconid on M1
    0: Protoconid taller than metaconid
    1: Subequal
    2: Metaconid taller than protoconid

53. Presence of paraconid on M2
    0: Absent
    1: Present
54. Distinctiveness of the M2 paraconid relative to the M1 paraconid
    0: Comparably distinct to the M1 paraconid
    1: Less distinct than the M1 paraconid
55. Relative height of the paraconid compared to the metaconid on M2
    0: Paraconid lower than metaconid
    1: Paraconid subequal of taller than metaconid
56. Relative height of the hypoconid compared to the entoconid on M2
    0: Hypoconid taller than entoconid
    1: Subequal
    2: Entoconid taller than hypoconid
57. Relative height of the protoconid compared to the metaconid on M2
    0: Protoconid taller than metaconid
    1: Subequal
    2: Metaconid taller than protoconid
58. Acuteness of cusps
    0: Relatively acute
    1: Blunter
59. Presence of M3 paraconid
    0: Absent
    1: Present
60. Relative height of the hypoconid compared to the entoconid on M3
    0: Hypoconid taller than entoconid
    1: Subequal
    2: Entoconid taller than hypoconid
61. Relative height of the protoconid compared to the metaconid on M3
    0: Protoconid taller than metaconid
    1: Subequal
    2: Metaconid taller than protoconid
62. M3 trigonid basin area
    0: Small basin, straight at the front
    1: Expansive trigonid basin, curved at the front
63. Morphology of the M3 hypoconulid lobe
    0: From a distal view, the central occlusal surface is taller than the sides
    1: from a distal view, the medial and later edges are taller than the central occlusal surface

Appendix B: Character Taxon Matrix Used in Phylogenetic Analysis

	1	2	3	4	5	6	7	8	9	10
Ignacius species 1	2	?	?	?	?	?	?	?	?	?
Ignacius species 2	2	1	0	1	?	?	?	?	?	?
I. frugivorus	0	1	0	0	1	1	1	0	1	2
I. clarkforkensis	0	?	0	1	0	1	1	?	0	2
I. fremontensis	0	1	0	0	?	1	1	0	1	2
I. graybullianus	0	?	?	?	?	1	1	1	0	2
Phenacolemur archus	0	1	1	0	?	1	0	1	1	2
Arcius fuscus	0	1	1	1	?	1	1	0	0	2
Arcius lapparenti	1	1	1	1	?	1	1	0	0	2
Arcius rougieri	0	0	0	1	0	1	1	0	0	2
Arcius zbyszewskii	0	?	?	?	?	1	1	1	0	2
Acidomomys hebeticus	1	2	0	0	1	1	0	?	0	?
Edworthia lerbekmoi	0	?	?	?	?	?	?	?	?	?
Paromomys farrandi	0	?	?	?	?	0	0	0	0	1
Purgatorius coracis	0	?	?	?	?	0	0	0	1	0
Torrejonia sirokyi	0	?	?	?	1	?	?	?	?	?
Chronolestes simul	0	?	?	?	1	0	0	0	0	1

	11	12	13	14	15	16	17	18	19	20
Ignacius species 1	?	?	?	1	0	2	0	0	0	1
Ignacius species 2	?	?	?	?	0	2	0	0	0	1
I. frugivorus	0	?	0	?	1	2	0	1	1	0
I. clarkforkensis	1	1	?	0	0	2	0	1	1	1
I. fremontensis	0	0	0	0	0	1	0	1	0	0
I. graybullianus	0	0	0	1	0	2	1	1	1	1
Phenacolemur archus	0	0	1	?	1	1	0	1	1	0
Arcius fuscus	1	1	0	?	1	1	1	0	1	?
Arcius lapparenti	1	1	0	?	1	1	1	0	1	0
Arcius rougieri	1	1	0	?	1	1	1	0	0	0
Arcius zbyszewskii	1	1	1	?	0	1	1	1	1	0
Acidomomys hebeticus	1	0	0	?	0	1	0	1	0	0
Edworthia lerbekmoi	?	?	?	?	?	?	?	?	?	?
Paromomys farrandi	1	1	0	?	0	0	0	1	0	0
Purgatorius coracis	0	0	0	?	0	0	0	1	0	0
Torrejonia sirokyi	?	?	?	0	0	0	1	1	0	0
Chronolestes simul	1	0	0	0	0	0	0	1	1	1

	21	22	23	24	25	26	27	28	29	30
Ignacius species 1	1	1	1	2	1	1	?	?	1	1
Ignacius species 2	1	1	0	0	0	1	0	2	1	1
I. frugivorus	0	1	1	0	1	0	1	1	1	1
I. clarkforkensis	1	1	1	0	1	?	0	2	1	1
I. fremontensis	0	3	0	0	1	0	1	1	1	1
I. graybullianus	0	1	0	0	1	1	0	2	1	1
Phenacolemur archus	0	?	0	0	0	0	?	?	1	1
Arcius fuscus	0	1	1	0	0	?	0	1	?	?
Arcius lapparenti	0	1	1	0	0	?	0	?	?	?
Arcius rougieri	0	0	1	0	0	0	0	?	1	1
Arcius zbyszewskii	?	1	0	1	0	?	0	?	?	?
Acidomomys hebeticus	0	1	0	0	1	0	?	?	1	1
Edworthia lerbekmoi	?	?	?	?	?	?	?	?	0	0
Paromomys farrandi	0	3	0	1	0	?	1	?	?	?
Purgatorius coracis	0	3	1	1	0	1	1	0	?	?
Torrejonia sirokyi	0	3	1	1	0	0	1	0	0	1
Chronolestes simul	0	0	1	1	0	0	0	0	0	0

	31	32	33	34	35	36	37	38	39	40
Ignacius species 1	1	?	?	?	?	?	?	?	?	?
Ignacius species 2	1	0	0	1	0	0	0	1	1	1
I. frugivorus	1	0	0	0	0	0	0	1	1	1
I. clarkforkensis	1	1	0	1	0	0	0	1	?	1
I. fremontensis	0	0	0	0	0	0	0	1	1	1
I. graybullianus	1	0	0	1	0	0	0	1	1	0
Phenacolemur archus	1	0	1	1	1	1	1	1	1	1
Arcius fuscus	?	1	?	0	0	?	?	0	1	1
Arcius lapparenti	?	1	?	0	0	?	?	1	1	1
Arcius rougieri	1	1	0	0	0	0	0	1	1	1
Arcius zbyszewskii	?	?	?	?	?	?	?	?	?	?
Acidomomys hebeticus	0	1	0	?	?	0	0	1	1	0
Edworthia lerbekmoi	0	1	0	0	0	0	0	1	0	1
Paromomys farrandi	?	1	?	0	0	?	?	0	0	1
Purgatorius coracis	?	?	?	?	?	?	?	?	?	?
Torrejonia sirokyi	0	1	0	1	0	0	0	0	0	1
Chronolestes simul	0	1	1	1	0	1	1	0	0	0

	41	42	43	44	45	46	47	48	49	50
Ignacius species 1	?	?	0	1	0	0	0	1	0	2
Ignacius species 2	0	1	1	1	0	0	0	1	0	2
I. frugivorus	0	0	0	1	0	0	0	0	1	2
I. clarkforkensis	0	0	0	?	0	0	0	0	1	2
I. fremontensis	0	0	1	1	0	0	0	0	1	2
I. graybullianus	0	0	1	1	0	0	0	0	0	2
Phenacolemur archus	0	0	1	1	0	0	1	1	0	1
Arcius fuscus	1	0	1	0	1	1	1	1	0	1
Arcius lapparenti	0	0	1	0	1	1	1	1	0	1
Arcius rougieri	0	0	1	0	1	1	1	0	0	0
Arcius zbyszewskii	?	?	1	?	0	1	1	0	?	1
Acidomomys hebeticus	0	2	1	1	0	0	0	0	0	1
Edworthia lerbekmoi	0	0	1	1	0	0	1	1	0	1
Paromomys farrandi	?	2	0	0	0	0	1	1	0	1
Purgatorius coracis	?	?	0	0	0	1	1	0	0	0
Torrejonia sirokyi	1	2	1	0	0	0	1	1	2	0
Chronolestes simul	1	2	1	0	0	1	0	0	2	0

	51	52	53	54	55	56	57	58	59	60	61	62	63
Ignacius species 1	1	2	1	1	1	2	2	1	?	?	?	?	?
Ignacius species 2	1	2	1	1	1	2	2	1	0	1	2	0	1
I. frugivorus	1	2	1	0	0	1	2	1	1	1	2	0	1
I. clarkforkensis	?	?	0	1	0	?	?	1	0	?	?	0	?
I. fremontensis	2	2	1	1	0	2	1	1	1	2	1	0	1
I. graybullianus	0	2	0	0	0	0	2	1	0	2	2	1	0
Phenacolemur archus	0	1	1	1	0	1	1	0	0	1	1	0	1
Arcius fuscus	0	1	0	?	?	0	1	0	0	0	1	1	0
Arcius lapparenti	0	1	1	1	0	1	1	0	0	0	1	1	0
Arcius rougieri	0	0	1	1	0	0	0	0	?	?	?	?	?
Arcius zbyszewskii	?	?	1	1	0	0	0	0	1	0	1	1	0
Acidomomys hebeticus	1	1	0	?	?	2	1	1	0	1	1	0	1
Edworthia lerbekmoi	0	0	1	0	0	2	1	0	1	0	0	0	1
Paromomys farrandi	1	0	1	0	?	1	1	0	1	1	0	0	0
Purgatorius coracis	0	1	1	1	0	1	0	0	1	1	1	0	0
Torrejonia sirokyi	1	1	1	1	0	0	2	0	1	0	2	1	1
Chronolestes simul	0	0	1	0	0	0	1	0	1	0	2	1	1

Appendix C: List of Individual Specimens and Dental Measurements

Lower p4 measurements (mm)		
Specimen #	**P/4 Width**	**P/4 Length**
CMN 30949	1.99	2.197
CMN 30837	1.991	2.236
CMN 30936	2.293	2.357

Lower m1 measurements (mm)		
Specimen #	**M/1 Width**	**M/1 Length**
CMN 30954	2.846	3.044
CMN 30864	3.021	3.289
CMN 30837	3.038	3.647
CMN 30828	3.159	3.629
CMN 30999	3.239	3.547
CMN 30986 (Sp. 1)	3.529	4.26

Lower m2 measurements (mm)		
Specimen #	**M/2 Width**	**M/2 Length**
CMN 30856	2.564	2.933
CMN 30864	3.232	3.67
CMN 30850 (Sp. 1)	3.998	4.677

Lower m3 measurements (mm)		
Specimen #	**M/3 Width**	**M/3 Length**
NMC 30889	3.089	5.007
NMC 30997	3.125	5.142
NMC 30933	3.129	-
NMC 30883	3.15	-
NMC 30902	3.253	-
NMC 30988	3.368	-

Upper I1 measurements (mm)		
Specimen #	**I1/ Width**	**I1/ Length**
CMN 30903	3.285	2.52
CMN 32325	3.707	2.068

Upper M1 measurements (mm)		
Specimen #	**M1/ Width**	**M1/ Length**
CMN 30996	3.735	3.113
CMN 32320	3.974	3.304
CMN 30995	4.025	3.165
CMN 30830 (Sp. 1)	5.14	4.112

Upper M2 measurements (mm)		
Specimen #	**M2/ Width**	**M2/ Length**
CMN 30998	3.535	4.28
CMN 30868	4.178	3.32

Upper M3 measurements (mm)		
Specimen #	**M3/ Width**	**M3/ Length**
CMN 32321	3.08	4.21

Mandibular depth measurements (mm)	
Specimen #	**Mandibular Depth**
CMN 30853 (edentulous)	7.928
CMN 30837	8.583
CMN 30835 (edentulous)	8.946
CMN 30986 (Sp. 1)	11.089
CMN 30850 (Sp. 1)	11.127